Effects of weather variation on waterfowl migration: lessons from a continental-scale generalizable avian movement and energetics model

Running title: Continental GAME model

Kevin J. Aagaard[1,*], Eric V. Lonsdorf[2], Wayne E. Thogmartin[3]

[1]Colorado Parks and Wildlife, 317 West Prospect Road, Fort Collins CO, 80526, USA

[2]University of Minnesota, Institute on the Environment, 1954 Buford Ave, St. Paul, MN 55108, USA

[3]U.S. Geological Survey, Upper Midwest Environmental Sciences Center, 2630 Fanta Reed Rd, La Crosse, WI 54603, USA

[*] Corresponding author email – kevin.aagaard@state.co.us

ABSTRACT

We developed a nonbreeding period continental-scale energetics-based model of daily waterfowl movement to predict year-specific migration and overwinter occurrence. The model approximates energy-expensive movements and energy-gaining stopovers as functions of metabolism and weather, in terms of temperature and frozen precipitation (i.e., snow). The model is a Markov process operating at the population level and is parameterized through a review of literature. We examined model performance against 62 years of non-breeding period daily weather data. The average proportion of available habitat decreased as weather severity increased, with mortality decreasing as the proportion of available habitat increased. The most commonly used nodes during the course of the nonbreeding period were generally consistent across years, with the most inter-annual variation present in the overwintering area. Our model revealed that the distribution of birds on the landscape changed more dramatically when the variation in daily available habitat was greater. The main routes for avian migration in North America were predicted by our simulations: the Eastern, Central, and Western flyways. Our model predicted an average of 77.4% survivorship for the nonbreeding period across all years (range = 76.4 – 78.4%), with lowest survivorship during the fall, intermediate survivorship in the winter, and greatest survivorship in the spring. We provide the parameters necessary for exploration within and among other taxa to leverage the generalizability of this migration model to a broader expanse of bird species, and across a range of climate change and land use/land cover change scenarios.

Key Words: Avian, energetics, global climate change, migration, predictive modeling, waterfowl

Introduction

Migratory behavior of populations varies within an avian species as well as among individuals within a population (Newton 2006, Newton and Brockie 2008, Eichhorn et al. 2009, Stanley et al. 2012). This differential migratory behavior is influenced by environmental change operating over ecological and evolutionary time scales (Parmesan 2006, Louchart 2008). Wide plasticity in migratory behavior is demonstrated by some individuals of a species initiating habitual seasonal migrations, with some foregoing migration to remain sedentary (Atwell et al. 2011). Understanding the mechanistic reasons for this difference in behavioral outcomes is critical to predicting responses of migratory populations to a changing environment.

Efforts to model avian migration from an energetic perspective have necessarily been informed by empirical biological and physiological studies (see Malishev and Kramer-Schadt 2021 for a review). For many species these empirical studies elucidated relationships between, for example: temperature and metabolism (e.g., Hartung 1967, Smith and Prince 1973, Klaassen 1996), body mass and temperature (e.g., Baldwin and Kendeigh 1938, Boos et al. 2007), and flight velocity and duration and body fat content (e.g., Rayner 1990). Using systems of equations to connect one facet to the next generates a series of expectations for how migration is likely to unfold for a bird of a certain species and specific mass (e.g., Lonsdorf et al. 2016, Aagaard et al. 2018). Connecting approaches for predicting environmental effects on migration-energetic dynamics with approaches evaluating the spatially explicit pattern of energetic-based migratory movements can reveal how migration is affected by the distribution of forage material on the landscape. It can also inform how migration is likely to proceed given the differential

expenditure of energy across the landscape and across temporally variable environmental conditions (Paxton et al. 2014).

While migration is a common term, we draw a distinction between it and movement and dispersal for consistency (Holloway and Miller 2017). Movement is any change in location over time. Dispersal is movement that occurs in spatially limited local communities without cyclical repetition (i.e., within a node, for our purposes; Ai et al. 2012). Migration is predictable or routine seasonal movement among two or more distinct and consistent habitats (Hansson and Åkesson 2014). Migratory birds are faced with several contrasting strategies along their journey relating to timing, distance, velocity, altitude, and stopover length (Alerstam and Lindström 1990). These dilemmas are captured in three tradeoffs: avoiding predation or refueling, flying at a speed allowing for maximum power or maximum range, and departing on migration early (to avoid inhospitable weather) or late (to further increase fat reserves) as opposed to "on time" (Pennycuick 1975, Alerstam and Lindström 1990, Hedenström 1992, Bruderer and Boldt 2001, Drent et al. 2003, Pennycuick and Battley 2003, La Sorte et al. 2013, Pennycuick et al. 2013). Each trade-off can be thought of as choice between different energetic or physiological strategies, essentially boiling down to 'full throttle' or 'fuel-efficient' transport. An easy analogy can be made between migrants and automobile drivers (Kitamura and Sperling 1987); depending on the nature of the trip, a driver may choose to optimize for automobile velocity or fuel efficiency. Migratory birds must make similar tradeoffs during the course of their movements. For a more complete elaboration of the ecological processes of avian migration, see, for example, Alerstam and Lindström (1990), Drent et al. (2003), Alves et al. (2013) and Aagaard et al. (2018).

We extend existing energetics-based models of waterfowl movement (Lonsdorf et al. 2016, Aagaard et al. 2018) to construct a full nonbreeding period model of waterfowl movement and energetics. Our model is of the type described by Malishev and Kramer-Schadt (2021) and referred to as an energetics-based Individual Based Model (eIBM); we note that the irreducible unit of interest in our models are more precisely considered "agents" rather than "individuals", as we follow subsets of the population but not discrete individuals. The model approximates energy-expensive movements and energy-gaining stopovers as functions of weather, in terms of air temperature, air density, and snow depth, which influence the timing and extent of waterfowl migration (Nichols et al. 1983). The model begins in the late summer/early autumn as birds are forced out of breeding habitat by inhospitable weather conditions. As in Lonsdorf et al. (2016) and Aagaard et al. (2018), we model bird movement as a function of the roosting quality and forage availability of each stopover site and the distance between the stopover site and departure site. We partition the population of birds into a set of body condition classes based on body mass and body fat. We transition birds among body condition classes based on differential movement and foraging, with the assumption of an inverse relationship between body condition and mortality risk.

We allow the bounds of the overwintering area to be an emergent property of the model rather than restrict it to static interpretations of historical overwintering grounds. We, therefore, add consideration of the distance from the stopover site to all other available stopover sites within an individual's flight range into our approximation of bird movement. We also consider the consequences of a seasonally varying availability of forage by accommodating the consumption and natural decay of forage material. Additionally, we impose thresholds related to known waterfowl abundance-weather severity relations (e.g., Schummer et al. 2010) to bird

105 movement to restrict availability of the landscape to only those sites with hospitable conditions
106 (Van Den Elsen 2016). Weather severity can be thought of as a propellant during the early
107 portion of the nonbreeding period to "push" birds southward, while the breeding grounds serve
108 as an attractant to "pull" birds northward. In this way, birds in this model tend to congregate
109 along a weather-severity isocline, staying as close to breeding grounds as weather conditions and
110 metabolic demands allow (e.g., Robinson et al. 2016).

111 While the model structure outlined here is generalizable to all birds, we use dabbling ducks
112 as an example (specifically, we parameterize our model for a mallard-like, *Anas platyrhynchos*,
113 dabbling duck). Mallards are exemplary model organisms in this context as they have been
114 extensively studied in terms of their physiology and migratory dynamics (e.g., Prince 1979,
115 Krementz et al. 2011, 2012, Pennycuick et al. 2013) and are of great conservation and
116 management interest (e.g., Heitmeyer 2010).

117 A critical advancement of this model is development of over 50 years of migration
118 trajectories using historical weather data to inform movement patterns, allowing sensitivity in
119 input parameter values to approximate observed conditions. With this model, we seek to
120 understand the influence of weather patterns and conditions on the nonbreeding period of the
121 annual cycle of migratory dabbling ducks. A full evaluation of this first-principles exposition of
122 avian migration requires broad-scale data revealing avian migration patterns associated with
123 historical environmental data. In the absence of such data we can at least use our approach to
124 determine if, all else being equal, variation present in a representative sample of observed
125 historical environmental conditions facilitates demonstrable changes to avian migration patterns
126 (Grim and Railsback 2012). Specifically, we expect (1) to determine explicitly and natively the
127 overwintering habitat; (2) past environmental data to provide evidence that climate change has

led to increased available habitat over time (and less severe weather); (3) a reduction in nonbreeding period mortality concurrent with an decrease in weather severity; (4) to recover migratory routes (flyways); and (5) to discern differences between mild and severe years comparable to historical weather reports.

Methods

We discretized the landscape (North America) into 1036 km^2 stopover sites, or nodes. This spatial delineation is consistent with expectations that movement less than 16 km consists of dispersal (Lonsdorf et al. 2016). Data availability and computational advancements allow us to greatly increase the temporal scale of the model relative to that considered in Lonsdorf et al. (2016): rather than focus on migratory jumps we iterate across each day of the nonbreeding period. As such, our model begins after the molting stage of waterfowl (1 September of one calendar year) and terminates prior to the breeding period (31 May of the following calendar year). We use known values from the literature for physiological, anatomical, and metabolic dynamics to inform our model (Table 1).

The workflow to simulate daily movement was constructed to most closely approximate the actual processes of movement, dispersal, and migration while operating under the constraints of a sequential modeling framework. Our pattern proceeded as:

Forage ⟶ Departure ⟶ Arrival ⟶ Mortality ⟶ Forage…

Within each component of our model there were secondary procedures invoked, for example, to effectively allocate forage material among individuals within the population and to distribute individuals across the landscape according to the spatial pattern of high-quality habitat. The

151 overall workflow is depicted in Figure 1. R code (R Core Team 2018) is available in Supporting
152 Materials File S1.

153 *(1) Forage*

154 A simulated day began with foraging, a weather- and body condition-dependent process,
155 which transfers energy from forage material on the landscape into energy as fat to individual
156 birds. Individuals in each node (distributed spatially according to NatureServe range maps
157 [Ridgley et al. 2005] and breeding population survey data) were allocated among 21 body
158 condition classes, with higher classes representing better body conditions. Body condition is a
159 function of body fat; individuals falling below body condition class one (into class zero) had 0%
160 body fat content (fatal). An individual's ability to accumulate forage—its rate of daily gain (*DG*)
161 —was a function of disturbance (degree of urbanization in a node), fuel deposition rate (*FDR*, kJ
162 per day), and temperature-dependent basal metabolic rate (Aagaard et al. 2018). We summed the
163 fuel deposition of each individual to calculate the amount of energy removed from the landscape
164 in each node as a result of active foraging.

165 To calculate the rate of natural decay (*D*) in forage material we multiplied the amount of
166 forage material (*E*, kJ) present in each habitat type (shoreline, crop, wooded wetland, herbaceous
167 wetland, Table 2) by a land cover-specific decay rate (*r*) to the power of the day of the
168 nonbreeding period (*i*):

169 $$D = E \times r^{i}.$$

170 We calculated the total forage available on the landscape in the next time step by subtracting the
171 amount of forage material subject to decay and active foraging from the total amount of forage
172 available (*F*) at the outset of day *i*,

173 $$F_{i+1} = F_i - D - \sum FDR.$$

174 *(2) Departure*

175 Each day, individuals must decide whether to stay and continue foraging or depart from a
176 node. We assumed that individuals in poorer body condition experiencing mild weather nearest
177 to breeding nodes with potential for high rates of gain of body mass were less likely to leave a
178 node, instead remaining to continue foraging, while individuals in better body condition facing
179 severe weather far from breeding nodes with potential for low rates of gain of body mass were
180 highly likely to leave. The probability of individuals remaining in a given node or departing from
181 it depends on each individual's body condition (*BC*), the weather severity index (*WSI*) within the
182 node, the distance between the origin node and the nearest breeding node (*DB*), and the
183 disturbance-dependent daily gain in body mass (*DG*). The components were combined according
184 to the follow equation:

185 $$\sum Pr(depart) = Pr(depart|WSI¿ + Pr(depart|BC¿ + Pr(depart|DB¿ + Pr(depart|DG¿.$$

186 Three of the four components, *BC*, *WSI*, and *DB*, were each calculated using a Monod function,
187 which produced a saturating curve for the target effect, with exponents applied to vary the shape
188 of the resulting curve. Daily Gain was calculated using a linear decreasing function. The discrete
189 probabilities of departure had the following forms:

190 $$Pr(depart|WSI) = \left(\frac{(WSI+7.5)^3}{(WSI+7.5)^3+(7.5)^3}\right),$$

191 $$Pr(depart|BC) = \left(\frac{BC^8}{BC^8+(N_{BC\,classes}-3)^8}\right),$$

192 $$Pr(depart|DB) = \left(\frac{DB^5}{DB^5+flight\,range^5}\right),$$

193 $$Pr(depart|DG¿ = \left(\frac{1-(FDR+1)}{5}\right).$$

194 The values for the exponents in each of these three cases were selected to generate
195 reasonable curves for each probability of departure component. We assessed what constitutes
196 "reasonable" based on the reaction in the model to changes in these values. We expected that the
197 curve for the body condition component should have a pronounced inflection point to represent a
198 high probability of departure for birds in the highest body conditions (top three), and a relatively
199 low probability of departure for birds in moderate to low body conditions. Weather severity, in
200 contrast, should be relatively more linear. Thus, we set the exponents in body condition to be
201 nearly three times as great as those in *WSI*.
202 More formally, we calculated the number of individuals departing each node as the product
203 of the abundance per node, i, on day, k, and the proportion of individuals in each BC, j; this
204 product was then multiplied by the BC-dependent probability of departure:
205
206 ¿
207
208 *(3) Arrival*
209 Once individuals choose to depart, they must decide how far to fly and where to land. How far
210 birds can fly is a function of body condition (mass, body fat proportion), flight cost, and flight
211 velocity. Using the relations set forth in the program Flight (for Windows, version 1.25
212 [http://www.bio.bristol.ac.uk/people/pennycuick.htm]; Pennycuick 2008), we calculated the
213 chemical power, velocity for maximum range, and effective lift-to-drag ratio for birds from a
214 distribution of available body masses, wing spans, wing areas, and at various air densities, across
215 a range of potential true air speeds. These calculations led to the ultimate output of the flight cost
216 (kg of fat metabolized per km) and flight velocity (km per hr), for the input range of

morphometric features. The code used to generate these calculations is included in Supporting Material File S4.

Birds determine where to land based on *WSI*, forage availability, roosting habitat, and distance to breeding grounds. On average, birds will tend to select more attractive nodes, that is, nodes with low winter severity (*WSI*) and higher air density (*AD*), plentiful forage availability and roosting habitat (*R*), nearer to breeding grounds, and within the flight range (defined as a node-specific gamma movement probability, *G*; the cumulative probability of moving from a node to all other nodes in the landscape based on the distance between each pair of nodes). We used a Cobb-Douglas function to combine these factors.

We restricted movement to nodes in which the *WSI* was below the empirically derived threshold (7.5; Schummer et al. 2010). The remaining four components of the arrival function (forage, roosting, breeding ground distance, gamma movement probability) were individually weighted to allow for the differential significance of particular parameters (w_f, forage availability; w_a, air density; w_r, roosting quality; w_b distance to nearest breeding node; and w_g, node-specific gamma movement probability). We also assumed variable relative importance of each component over time (Figure 2). We assumed that distance to the nearest breeding node was the most important consideration for migrants proximal to the breeding period (i.e., early and late in the nonbreeding period). We assumed that forage availability and roosting quality increased in importance up to the mid-winter period of the nonbreeding period—with forage increasing more so than roosting—and then decreased to initial values again by the end of the nonbreeding period. We held the node-specific gamma movement marginal probability steady across the nonbreeding period because the probability of moving between any given pair of nodes (depending only on the distance between them) should not vary temporally.

240 Input values for the component weights were, for w_f, 0.45 , w_a, 0.3, w_r, 0.2, and w_g, 0.05.
241 The weight for the distance to breeding grounds, w_b, was set to the sum of the daily weights for
242 all other components subtracted from one. To establish the structure of the weights for the
243 components assumed to have non-linear dynamics we randomly selected a date during the mid-
244 winter phase of the nonbreeding period (between 31 December and 31 January) to serve as our
245 inflection point. We then generated a sequence of values, *c*, from 1 to 0.1 to 1, with an inflection
246 occurring on the specified day of the nonbreeding period, *d*, for use in a function to calculate the
247 corresponding weights for each component:

248 $$w_f = -\left(0.9 \times \left(\left(c_d - \left(\frac{c_d}{n}\right)\right)^2\right)\right) + 0.45$$

249 $$w_a = -\left(0.6 \times \left(\left(c_d - \left(\frac{c_d}{n}\right)\right)^2\right)\right) + 0.3$$

250 $$w_r = -\left(0.4 \times \left(\left(c_d - \left(\frac{c_d}{n}\right)\right)^2\right)\right) + 0.2$$

251 $$w_g = 0.05$$

252 $$w_b = 1 - \sum \left(w_f, w_a, w_r, w_g\right),$$

253 where *n* is the length of the nonbreeding period in days.
254 Using this process to generate the daily weights, the full Cobb-Douglas function for the
255 probability of arrival in a given node was defined as:

256 $$A = F^{w_f} \times AD^{w_a} \times R^{w_r} \times DB^{w_b} \times G^{w_g}.$$

257 Each of these components was normalized to a 0-1 scale, using $\frac{x - min\,(x)}{min(x) - max\,(x)}$; the node with
258 the greatest amount of forage availability on a given day was assigned a normalized forage

availability score of 1; we repeated this calculation for roosting quality, distance to nearest breeding node, and node-specific gamma movement probability.

(4) Mortality

We assumed that individuals in poorer body conditions had higher daily rates of mortality than individuals in better body conditions—in keeping with the assumption of increased mortality with increased energy deficits (e.g., Lonsdorf et al. 2016). Each day we multiplied the survivorship associated with a given body condition by the number of individuals in that body condition class.

Daily Abundance – We redistributed individuals across the landscape and among body condition classes according to their probabilities to stay/depart and arrive. We calculated the following day's abundance in a node as the product of the total number of individuals departing all nodes and the probability of arrival in the node:

¿ = ¿,

added to the difference of the current abundance and the number of individuals departing the node.

We computed the number of individuals departing a node in each body condition and the number of individuals remaining in a node in each body condition. We decremented the body condition of departing individuals according to the distance between origin-node and destination-node, using established relations for the mass-dependent cost of flight per unit distance (e.g., see Aagaard et al. 2018). This decrement-function informed the number of individuals arriving in

each node in each body condition, which we used to calculate the number of individuals in each node in each body condition class on the following day.

The final abundance for a given node on the following day was the abundance in that node on the current day minus the number of individuals that died in that node on that day. Taken together with *Arrival*, this produced:

¿.

Parameterization – For some parameters in our model there is a lack of empirical evidence to inform their value. We defined these parameters probabilistically, as a function of body condition, to allow for sensitivity in the model (Table 1; see also Appendix S1 for definitions of parameters and distributions). These included daily survivorship, flight power components, and energetic costs of flight. We also allowed parameters with known individual variation to vary within the population, such as flight velocity, body mass, and proportion of body mass composed of metabolizable lipids. We applied these distributions to the starting population of ~20 million birds and updated the fluctuating variables according to incurred energetic costs (body mass, available metabolizable lipids). This arrangement allowed us to capture a realistic representation of the distribution of realized values for each parameter in the model without unreasonably increasing computing time. We varied the parameter values associated with the prior distributions for morphological features to evaluate their effects on the model (monitoring estimated survivorship as a comparison point), including daily survivorship, flight power components, morphological components, and energetic components.

(1) Daily Survivorship

Daily survivorship ranged from 0.99620 to 0.99984, from the second body condition bin to the optimal body condition bin (body condition bin 1 represented dead individuals, survivorship = 0). We assumed birds that exceeded some critical mass would experience heightened mortality as a result of increase predation risk (or decreased predation avoidance ability), in keeping with optimal body mass theory (Lima 1986). We therefore set the optimal body mass to be that of a 1.625 kg bird (~0.134 kg of fat), about the maximum of observed mallard body masses in the field (Owen and Cook 1977; while noting and allowing for the rare occurrence of heavier birds).

(2) Flight power components

Air density was informed by measured and interpolated air pressure values, as detailed in Appendix S1. The absolute range in air density across the period of sampled data was 0.95 to 1.3 $\frac{kg}{m^3}$. The true air speed – that is, the velocity at which molecules *appear* to move past a moving body from the perspective of the body in motion – ranged from 10 to 25 $\frac{m}{s}$. Flight velocity (the actual velocity of the body in motion) ranged from 75.92 to 87.37, according to relations laid out in Flight (for Windows, version 1.25 [http://www.bio.bristol.ac.uk/people/pennycuick.htm]; Pennycuick 2008).

(3) Morphological components

Body mass, wing span, and wing area were all modeled to follow skew-normal distributions with $\mu = 1.2$ and $\sigma = 1.21$ [body mass], $\mu = 0.95$ and $\sigma = 1$ [wing span], and $\mu = 0.1$ and $\sigma = 0.1$ [wing area] (Owen and Cook 1977; assuming most individuals begin migration only when closer to optimal body condition). The proportion of body mass composed of metabolizable lipids (*kg*) was set to 11%, and was subsequently allowed to vary from 8 to 14% (using values from Dabbert

et al. 1997, Boos et al. 2007). Lipids account for ~81% to 84% of metabolizable energy (Boos et al. 2007). Not all lipids are available for metabolic processes (some retained for other purposes, not detailed; Boos et al. 2002, 2007). We assume the ~16% to 19% of metabolizable energy provided by sources other than lipids is used for processes other than flight (basal metabolic rate, reproductive organs, cellular replacement, etc.). Therefore, we assume that all energy directed toward powered flight relies on lipids as its source exclusively, and not all the ~10% to 16% of body mass comprised of lipids is available for powered flight processes.

Body mass had a mean of 1.2 *kg* (Owen and Cook 1977, Pennycuick 2008). This resulted in a distribution with a range of 0.5 to 2 *kg*. Wing span and wing area had ranges of 0.75 to 1.15 *m* and 0.09 to 0.11 m^2 (respectively; Bruderer and Boldt 2001).

(4) Energetic components

The cost (*kg* of body fat) per unit distance flown (*km*) ranged from 2.1×10^{-5} to 1.6×10^{-4}, according to relations laid out in Flight (Pennycuick 2008). Without clear guidance from the literature to inform a consistent relationship between fuel deposition rate and climatic factors, we defined the coefficient of fuel deposition rate as a multiple of body mass and set it to 1.1% initially, and subsequently set it to 0.5 and 2 to represent low and high values. This arrangement is in line with values presented by Lindström (2003), in which the maximum fuel deposition rate for a ~1 kg non-passerine bird caps out at 2% of the lean mass, with a minimum of 0.3%.

Migration paths – For each year of the simulation we recorded a migration "path" – an approximation of the median route taken by the population during the nonbreeding period. We computed the abundance-weight center-of-mass for the population on each day; given the spatial distribution of individuals within nodes across the landscape, we identified the point representing

349 the centroid of the population (Figure 3). By tracking the latitude of this point each day we
350 assembled a trajectory representing the latitudinal and longitudinal shift of the centroid of the
351 population throughout the nonbreeding period. Evaluating the nadir of the latitudinal shift across
352 years informs potential temporal patterns in migration and overwintering dynamics. For
353 example, one might expect a general northward regression of the southern-most point of the
354 population center-of-mass through time as average global atmospheric temperatures increase
355 (Aagaard et al. 2018). Alternatively, the southern-most point might be more closely related to
356 weather severity, with a changing climate leading to increasingly variable weather patterns from
357 one year to the next; as such, there may not be a consistent decrease in severe weather but rather
358 more frequent extremes (more unusually mild and unusually severe weather years). By
359 regressing the southern-most point of the population center-of-mass with year and *WSI* we can
360 potentially parse this difference.
361 We calculated the mean distance between all consecutive population centers-of-mass, as well
362 as the distance between the northern-most and southern-most population centers-of-mass. These
363 metrics informed the mean distance moved by the population from one day to the next, as well as
364 the separation between breeding grounds and overwintering habitat. We identified the most
365 commonly used nodes during the course of the nonbreeding period by measuring the total
366 abundance in each node on each day to compute the top 2% most populace nodes per day. We
367 used these metrics to produce animations for each year of the record showing the daily,
368 normalized (0-1) abundance for each node in the landscape.

369

370 *Data sources* – Our model takes as input six data layers relating to habitat state and weather
371 conditions. There are five layers relating to habitat state; the first was derived from National

372 Land Cover Database (NLCD) 2006 for the USA (Fry et al. 2011) and the CSC2000v for Canada
373 (*available online*; see Appendix S2) to estimate roosting and foraging quality. We used
374 NatureServe range maps (Ridgley et al. 2005) to identify potential starting locations among
375 which to distribute birds at the onset of the nonbreeding period. We used these input layers in
376 conjunction with breeding population survey data (U.S. Fish and Wildlife Service 2013) to
377 establish abundance at breeding sites by weighting the total number of birds by the quality of
378 habitat within the site and the breeding population survey results for the area. We relied on daily
379 climate data from the National Oceanic and Atmospheric Association's National Centers for
380 Environmental Prediction National Center for Atmospheric Research Reanalysis Project (NOAA
381 NCEP; Kalnay et al. 1996).
382 We considered sites with a higher proportional area of shoreline, herbaceous wetlands, and
383 wooded wetlands to be of higher quality for roosting. In this fashion, breeding sites of high
384 quality aligning with large numbers of birds from the breeding population survey hosted the
385 greatest numbers of individuals. We estimated mean forage availability per site (in 0.1 GJ units)
386 at the outset of the nonbreeding period based on an evaluation of land cover using a range of
387 parameter estimates. Further details of this process, and the values used for the forage
388 availability parameter estimates, are available in Lonsdorf et al. (2016).
389
390 *Landscape generation* – Mallards have documented preferences for wetlands with shallow water
391 (5–20 cm) in which to forage and near which to roost (Colwell and Taft 2000, Guillemain et al.
392 2000). We classified shoreline cover as optimal roosting habitat (i.e., with a value of 1, while all
393 other cover types are 0), and calculated the proportion of each node occupied by shoreline cover.

394 Multiplying this proportion by the area of the focal node yielded the value of roosting quality
395 provided by that node.
396 We multiplied the amount of forage provided by each land cover type represented within the
397 node (using food-habit information from the literature; see Lonsdorf et al. 2016) by the
398 proportion of the node classified as each land cover type. We multiplied this value by the
399 proportion of forage *available* in a node, based on the distance to the nearest roosting site. Areas
400 in which forage and roosting habitat were nearby had greater proportions of their forage
401 available for consumption to account for a decrease in net energy extracted from a node given
402 the increased distance traveled to the foraging sites within the node. We multiplied this roosting
403 distance- and area-dependent forage availability measure by the area of the node to calculate the
404 quantity of forage available in each node (Pearse et al. 2012, Beatty et al. 2014).
405
406 *Winter severity* – To quantify the severity of the weather in a given node (and thus the
407 probability that birds will occupy that node), we followed the framework of Schummer et al.
408 (2010) wherein a weather severity index (*WSI*) was calculated based on the depth of snow in a
409 node (*S*, cm), the number of consecutive days with snow depth ≥2.54 cm (S_{days}), the temperature
410 in a node (*T*, °C), and the number of consecutive days with temperature <0 (T_{freeze}). The
411 formulation follows:
412 $$WSI = (S \times 0.394) + S_{days} + (-T) + T_{freeze}.$$
413 Schummer et al. (2010) found that the rate of change of the relative abundance at a location
414 switched from positive to negative when *WSI* = 7.5; we invoked this value as the threshold below
415 which individuals were expected to remain in a node and above which individuals were expected
416 to depart.

Model evaluation – We monitored a suite of metrics as we iterated our simulation across years to evaluate the degree to which migratory patterns differed annually. We monitored nonbreeding period mortality ($N_0 - N_n$; n is the last day of the nonbreeding period). We also monitored landscape availability, based on the number of nodes in which the *WSI* was less than the threshold each day. We calculated the mean availability (and standard deviation) of habitat, as well as the minimum availability at any point during the nonbreeding period. These values informed the average weather severity across the nonbreeding period, and the severity of the weather during the least hospitable portion of the nonbreeding period. We ran the model in R (R Core Team 2018).

Results

Objectives – As expected, we observed weather patterns and conditions effecting the nonbreeding period of the annual cycle of migratory birds. We were able to discern overwintering habitat as an emergent property of the model (Figure 3). The average proportion of available habitat (*WSI* < 7.5) across the landscape increased as winter weather severity decreased (Figure 4A), and mortality decreased as the proportion of available habitat increased (Figure 4B). Unexpectedly, mortality did not demonstrate any correlative trend with weather severity (Figure 4C), perhaps because birds flew beyond the range of the affected area. Importantly, whereas we summarized weather severity across the entire landscape, there was spatial heterogeneity in the variation of weather severity. The summarized *WSI* in the available habitat showed a slight increase over time, with a few years of above-average weather severity

later in the record (especially 2009-2010 and 2010-2011). However, the summarized *WSI* across the entire landscape decreased more dramatically over the same timeframe (even 2009-2010 and 2010-2011 produced below-average *WSI* scores) (Figure 5). We plotted the standard deviation of the mean annual *WSI* for each node across the period of record to demonstrate this point (Figure 6).

We were successful in our attempt to recover the primary avenues for migration (Figure 7 and File S4): a heavily-used central flyway along the Mississippi River, a well-defined Atlantic Flyway east of the Appalachian Mountains, and a disjointed Pacific Flyway along the west coast. The flyways tended to converge within the Prairie Potholes Region and along the southern shore of Hudson Bay (which is the NatureServe defined breeding region). The most commonly used nodes during the course of the nonbreeding period were generally consistent across years (Figure 7). The center-of-mass of the population during the migratory periods were similarly consistent across years, while the overwintering period showed more inter-annual variation (Figure 7). Finally, the model yielded strong evidence of the effect of *WSI* on the distribution of birds on the landscape. The mean distance among all daily center-of-mass locations was highly correlated with the standard deviation of available habitat (adj.-$R^2 = 0.86$; Figure 8), suggesting that the distribution of birds on the landscape changed more dramatically when the variation in daily available habitat was greater.

Temporally, we were able to distinguish between severe and mild years by their mean daily *WSI* values across the landscape, and the years identified as severe or cohered to historical weather anecdotes. We found that years with severe weather yielded correspondingly reduced available habitat during the winter months (Figure 10). Finally, we found that as *WSI* increased,

462 the population moved farther south during the nonbreeding period as available habitat was
463 reduced (Figure 10, and see Appendix S3).
464
465 *Validation* – Our model predicted an average survivorship of 77.4% for the nonbreeding period
466 across all years (range = 76.4 – 78.4%). This value is decomposed into an average survivorship
467 rate of 91.3% for the autumn migratory period (1 September to 30 November; 90.5 – 92.1%),
468 91.8% for the overwintering period (1 December to 28 February; 91.1 – 92.6%), and 92.4% for
469 the spring migratory period (1 March to 31 May; 91.5 – 92.9%). Mean daily mortality across the
470 period of record ranged from 13,100 to 21,000 birds (Figure 9). These estimates are
471 commensurate with literature-derived mortality estimates (Zimmer et al. 2010, Davis et al.
472 2011).
473
474 *Parameter sensitivity* – The proportion of birds in different body condition bins varied most
475 strongly at lower classes, with a two-order of magnitude increase in the proportion of birds in the
476 lowest body condition (starvation) over the nonbreeding period, and a 20% reduction in birds in
477 the top body condition. Decreasing the proportion of metabolizable body fat to 8% resulted in
478 survivorship (averaged across all years) of 86.72% (85.87 – 87.37%), whereas increasing it to
479 14% metabolizable body fat yielded survivorship of 50.66% (50 –51.35%). Increasing the
480 coefficient for the fuel deposition rate to 2 increased survivorship to 89.15% (89.05 – 89.22%),
481 whereas decreasing it to 0.5 decreased survivorship to 41.03% (39.99 – 41.95%) (while holding
482 the proportion of metabolizable body fat steady at 11%).
483
484 **Discussion**

485

486 We elaborated an energetics-based model of avian migration to more fully realize the stochastic
487 variation in migration induced by daily weather. Our model was able to recreate documented
488 North American avian migration routes (La Sorte et al. 2014a, La Sorte et al. 2014b, Lonsdorf et
489 al. 2016) and recover expected rates of survivorship (Lonsdorf et al. 2016; 90.5 ± 1.35% [mean ±
490 confidence interval] survivorship in autumn, 93.6 ± 1.1% survivorship in spring) based on
491 nothing more than first-principle arrangements of dabbling duck energetics and behavior. With a
492 thorough literature review and carefully considered parameterization, the model we present here
493 can be generalized to any migratory bird species. Extending the model to the entirety of the
494 nonbreeding period is a crucial step on the path to developing a generalizable energetics-based
495 full-annual-cycle model (Marra et al. 2015). We included consideration of weather severity on
496 the movement patterns of migrants, allowing us to form initial expectations about the role
497 climate and climate change can play in altering physiology and subsequent migration behavior
498 (Notaro et al. 2016). We introduced a refined forage availability scheme by allowing for
499 consumption and natural decay of forage material during the nonbreeding period.
500

501 *Interpreting results* – Our model suggests that the milder conditions across North America
502 resulting from climate change (Appendix S3; Schummer et al. 2017) are increasing the
503 proportion of habitat available to dabbling ducks which has led to decreased environmentally
504 induced mortality. This result is evident in the decrease in *WSI* over time across the continent,
505 demonstrating generally less severe winters over the period of record. This result is also
506 evidenced in the relationship between *WSI* and the minimum proportion of available habitat, with
507 less available habitat in years with greater *WSI*.

508 Walther et al. (2002) indicated that freeze-free periods were lengthening and that snow cover
509 has decreased since the 1960s. If these trends continue, as recent studies suggest (Notaro et al.
510 2014), we may expect to see more northerly overwintering (Abraham et al. 2005, Link et al.
511 2006, Tingley et al. 2009, Notaro et al. 2016). Taken to the extreme, this development may
512 suggest that mallard-like dabbling ducks could be approaching a cessation of migration (Moore
513 2011, Notaro et al. 2016, Aagaard et al. 2018). Recent studies investigating the changing patterns
514 of avian migration under the influence of climate change provide corroborating evidence of this
515 possibility (Walther et al. 2002, La Sorte and Thompson 2007); American black ducks (*Anas*
516 *rubripes*), for instance, have shown a tendency to remain in the region in which they breed
517 during migration, and some occasionally move in directions antithetical to conventional
518 migratory movements (Brook et al. 2009, Robinson et al. 2016). Whether this movement
519 represents inexperienced birds or the influence of climate or land use/land cover change has not
520 been decisively determined, but mounting evidence of similar patterns paired with the findings of
521 this and other simulation models suggest it is the latter.
522 By varying the proportion of available metabolizable body fat we were able to identify
523 sensitivity within the model. The effect of modifying the proportion of available metabolizable
524 body fat was counterintuitive; increasing body fat functionally increases available fuel and
525 should decrease time spent migrating, the most energy expensive aspect of the nonbreeding
526 period. However, the proportion of body fat does not influence the cost of flight, so two
527 individuals of the same body mass but different body fat proportions will be subjected to the
528 same energetic costs. The individual with a greater proportion of body fat will be able to travel
529 farther, decreasing its body mass more substantially and (based on the structure of our model)

530 subsequently transitioning into a lower body condition class with a lower associated daily
531 survivorship.
532 Given the harsher conditions and limited habitat availability during the overwintering period
533 (see Appendix S3), the lower survivorship is expected. In autumn, we expect greater forage
534 availability on the landscape than in winter (and possibly even spring), as seed and waste grain
535 has not yet decayed (Hagy and Kaminski 2012), so we expected higher survivorship during this
536 period. However, the timing of energy expensive migration fell in the autumn period (1
537 September to 30 November), which led to greater reductions in body condition and therefore
538 generally greater mortality rates. The higher mean survivorship rate of spring is likely a result of
539 less intense weather severity than in either the fall or nonbreeding periods.
540 When reviewing extreme weather events within the period of record we considered, there is
541 appreciable concordance with *WSI* and observed extremes (e.g., deep freezes in the south, as in
542 1957-1958, and 1961-1962). Events such as these, coupled with our model results, offer support
543 for the claim that poor weather tends to push birds farther south in search of hospitable habitat
544 (Figure 9). Conversely, mild years (such as 2015-2017) provide more available habitat across the
545 landscape (Figure 9), likely leading to the population generally staying closer to the breeding
546 grounds and demonstrating more willingness to withstand brief inclement weather, with the
547 expectation that more hospitable conditions await after it quickly passes. As climatic conditions
548 increase in variability this change could have dramatic effects on migratory dynamics, as some
549 years may see birds move only a short distance from the breeding grounds, while in other years,
550 comprised of extreme weather events, birds may be pushed relatively far south. If the tendency
551 of waterfowl is to remain sedentary as extreme events pass through, and if these events end up
552 lasting longer, this sedentary inclination could lead to unusually high mortality events in some

553 years. Historical data show a clear divergence in the spatial variation in weather severity,
554 consistent with expectations of increasingly extreme weather as the climate changes, so
555 predictions of general trends will necessarily be obscured by these spatially inconsistent weather
556 pattern changes.

557 Waterfowl enthusiasts (e.g., birders and hunters, Cooper et al. 2015) contribute >$100
558 million annually to the economies of Canada and the U.S. (Mattsson et al. 2018, 2020). Should
559 migration distance continue to shorten and sedentary behavior increase, the availability of
560 waterfowl to birders and hunters would likely be affected, potentially leading to decreased
561 funding in support of wetland habitat conservation (Grado et al. 2001, Cooper et al. 2015, López-
562 Hoffman et al. 2017). If hunter behavior were to change in response to differing migratory
563 patterns, the distribution of monetary resources would likely change as well (López-Hoffman et
564 al. 2017, Bagstad et al. 2018, Mattsson et al. 2020).
565
566 *Future research directions* – Our model has many important strengths in terms of advancing our
567 understanding of avian nonbreeding movement patterns within the context of energetics and
568 weather. We sought to maintain flexibility in the model for ease of adding components that
569 might increase the power of the model. We did not add these components in the present iteration
570 because, in some cases, there remain critical gaps in our knowledge requiring further research.
571 For example, while we included a placeholder for harvest-induced mortality, an important aspect
572 of migration dynamics (Klaassen et al. 2005, Vaananen 2001), we lacked access to data at the
573 relevant spatial scale to inform the effect of this source of mortality across the landscape. Efforts
574 to aggregate such data for inclusion in future iterations of this model would be extremely useful.

575 Because waterfowl migration is mediated on a daily time-step via weather, predicting waterfowl
576 availability on time horizons useful to hunters could be possible.
577 While we used pertinent land cover data to inform forage availability across the landscape,
578 we are aware of limitations in converting land cover classes into available kilojoules, as well as
579 grouping potentially distinct land cover classes into broad categories (Malishev and Kramer-
580 Schadt 2021). Targeted research into the seasonally varying availability of accessible forage
581 (including invertebrates) in various land cover classes is necessary to better inform this aspect of
582 the model (e.g., Fredrickson and Reid 1988, Kaminski et al. 2003, Bishop and Vrtiska 2008,
583 Beatty et al. 2017). Improving the reliability of spatial data layers is of particular importance to
584 eIBMs, given the significance of this input on the resulting dynamics predicted by the model
585 (Malishev and Kramer-Schadt 2021). Similarly, despite formatting our model with an agent-
586 based rather than individual-based framework, we ignored another main challenge eIBMs face
587 (Malishev and Kramer-Schadt 2021): accounting for complex behavior and movement (e.g.,
588 sociality and predation avoidance). Refining our understanding of the probabilistic tendencies of
589 individuals to alter movement dynamics as a function of social dynamics or predation threat
590 would greatly improve our approximation of especially small-scale (short-distance) movement.
591 In other cases, we omitted potentially important components because the complexity they
592 add to the model significantly inflates computational time. We foresee a framework for adding in
593 additional components in a serial, stepwise process. That is, we first developed a generalizable
594 energetics-based landscape model for avian migration (Lonsdorf et al. 2016), then laid the
595 foundation for the interaction between temperature and migration energetics (Aagaard et al.
596 2018), and now merge those efforts to generate a generalizable continental-scale energetics-
597 based landscape model of avian migration accounting for variable temperature and weather

598 severity and their effects on migratory dynamics. By building toward the ultimate goal of a fully
599 generalizable and energetics-based *animal* movement model one block at a time we provide a
600 cogent work flow and fully elaborate the logic at each step. Thus, we have for now ignored the
601 effect of some aspects such as wind direction on avian migration dynamics, a component known
602 to be predictive of movement patterns (La Sorte et al. 2014b). Adding model functions and data
603 relating to daily wind currents and velocity would likely improve the realism of our model and
604 provide refined predictions for migration routes and critical habitat areas (Gutierrez Illan et al.
605 2017).
606 We also excluded competition (Eichhorn et al. 2009, Stirnemann et al. 2012) and
607 epidemiological effects (Gilbert et al. 2006) from the model. While we found that *WSI* has
608 generally increased over time and led to decreased mortality, it is possible that altered disease
609 dynamics may counteract these gains in survivorship (i.e., as the climate becomes milder, disease
610 transmission may increase; Harvell et al. 2002), while decreased competition may provide the
611 opposite influence. Developing techniques to account for these dynamics in the model would be
612 beneficial. As with all models, we must balance realism in the model with the usefulness of the
613 general trends and predictions of the model.
614 Lastly, we made preliminary connections between the body condition of birds at the end of
615 the nonbreeding period and the energy available for reproduction during the breeding period.
616 Assuming an energy conversion of 39,700 kJ per kg of body fat (Rayner 1990), and an energy
617 content of 400 to 636 kJ per egg (636 kJ in Ricklefs 1977; 487 kJ in Sotherland and Rahn 1987;
618 400 kJ in Alisauskas and Ankney 1992), we estimate that, for 400 kJ per egg, only birds with
619 body mass greater than 0.725 kg and above would have sufficient fat reserves available at the
620 outset of the breeding period to lay at least one egg, and for 636 kJ per egg, only birds with body

mass greater than 0.8 kg would be able to lay at least one egg (see Krapu 1981 for discussion of body condition and breeding period success). Given a clutch size range for mallards of eight to 13 eggs (Drilling et al. 2020), we estimate that only birds with body mass over 1.4 kg (for 400 kJ per egg) or over 1.625 kg would lay a full clutch of eggs at the beginning of the breeding period. Birds in lower body conditions would need more time to forage to restock fat reserves sufficiently to produce a full clutch size. The modeled distribution of birds in each body condition at the end of the nonbreeding period indicates that approximately 3% (for 636 kJ per egg) to 15% (for 400 kJ per egg) of the population could effectively lay a standard size clutch of eggs at the beginning of the breeding period, also allowing for the possibility of a second clutch (depending on the size of each) later in the breeding period given a rapid enough rate of fuel deposition.

Conclusions – Accelerating change to land cover and climate is eroding avian migration as we know it. Merging environmental conditions with spatially explicit models of energetics-based migratory movements is helping to inform how the landscape affects migration patterns. Our model approximates avian migration during the nonbreeding period and the movement occurring among local stopovers along the way. Our results indicate that available habitat during the non-breeding period has likely increased over time, indicative of milder conditions as a product of a changing climate, ultimately leading to decreased (environmentally induced) mortality. This finding has important ramifications: if migration distance continues to diminish and the tendency for sedentary behavior increases, we may see altered hunter harvest across the landscape. Additionally, if sedentary behavior in the face of extreme events continues then birds may experience unusually high mortality events in some years. All these possibilities underscore the

644 need for continued advancements in the vein of this model to further illuminate the consequences
645 of a changing environment on avian migration.
646
647 **Acknowledgments**
648 We thank W. Beatty for providing several key enhancements to this manuscript. We appreciate
649 code scrutiny by B. West. We also thank V. Hunt for consultations and critical comments on
650 prior versions of this manuscript. Model development was aided by discussions with S. Jacobi
651 and M. T. Jones. Any use of trade, product, or firm names are for descriptive purposes only and
652 do not imply endorsement by the U.S. Government.
653
654 **Data Accessibility**
655 All data are stored in publicly available repositories as cited in the paper (e.g., weather data
656 comes from the National Oceanic and Atmospheric Administration's National Centers for
657 Environmental Prediction). We provide all code as Supporting Information, and the code has
658 annotated references to each data set.
659
660 **Literature Cited**
661 Aagaard, K., Thogmartin W. E., Lonsdorf E. V. (2018). Temperature-energy relations in
662 migratory waterfowl. *Ecological Modelling*, *378*, 46–58.
663 Abraham, K. F., Jefferies, R. L., & Alisauskas, R. T. (2005). The dynamics of landscape change
664 and snow geese in mid-continent North America. *Global Change Biology*, *11*(6), 841–855.
665 https://doi.org/10.1111/j.1365-2486.2005.00943.x

666 Ai, D., Desjardins-Proulx, P., Chu, C., & Wang, G. (2012). Immigration, local dispersal
667 limitation, and the repeatability of community composition under neutral and niche
668 dynamics. *PLoS ONE*, *7*(9), e46164. https://doi.org/10.1371/journal.pone.0046164
669 Alerstam, T., & Lindström, Å. (1990). Optimal bird migration: the relative importance of time,
670 energy, and safety. In Bird Migration (ed. E. Gwinner), pp. 331–351. Springer-Verlag,
671 Berlin, Germany. https://doi.org/10.1007/978-3-642-74542-3_22
672 Alisauskas, R.T. & Ankney, C.D. (1992). The cost of egg laying and its relationship to nutrient
673 reserves in waterfowl. In Ecology and management of breeding waterfowl (eds. B. Batt, A.
674 D. Afton, M. G. Anderson, C. D. Ankney, D. H. Johnson, J. A. Kadlec, and G. L. Krapu).
675 University of Minnesota Press, Minneapolis, pp.30-61.
676 Atwell, J. W., O'Neal D. M., Ketterson E. D. (2011). Animal as a moving target for
677 conservation: intra-species variation and responses to environmental change, as illustrated in
678 a sometimes migratory songbird. *Environmental Law (Northwestern School of Law)*, *41*,
679 289–316.
680 Bagstad, K. J., Semmens D. J., Diffendorfer J. E., Mattsson B. J., Dubovsky J., Thogmartin W.
681 E., Wiederholt R., Loomis J., Goldstein J., Bieri J. A., Sample C., López-Hoffman L. (2018).
682 Ecosystem service flows from a migratory species: spatial subsidies of the northern pintail.
683 *Ambio*, https://doi.org/10.1007/s13280-018-1049-4
684 Baldwin, S. P., & Kendeigh, S. C. (1938). Variations in the weight of birds. *The Auk*, *55*(3), 416–
685 467. https://doi.org/10.2307/4078412
686 Beatty, W. S., Webb, E. B., Kesler, D. C., Raedeke, A. H., Naylor, L. W., & Humburg, D. D.
687 (2014). Landscape effects on mallard habitat selection at multiple spatial scales during the
688 non-breeding period. *Landscape Ecology*, *29*, 989–1000.

689 Beatty, W. S., Kesler, D. C., Webb, E. B., Naylor, L. W., Raedeke, A. H., Hurnburg, D. D.,
690 Coluccy, J. M., and Soulliere, G. J. (2017). How will predicted land-use change affect
691 waterfowl spring stopover ecology? Inferences from an individual-based model. *Journal of*
692 *Applied Ecology*, *54*, 926-634. https://doi.org/10.1111/1365-2664.12788

693 Bishop, A. A., Vrtiska M. (2008). Effects of the Wetlands Reserve Program on waterfowl
694 carrying capacity in the Rainwater Basin Region of south-central Nebraska. *Natural*
695 *Resource Conservation Service*, https://www.nrcs.usda.gov/Internet/FSE_DOCUMENTS/16/
696 nrcs143_022300.pdf (Accessed 5 May 2017).Boos, M., Zorn, T., Delacour, G., & Robin, J.-
697 P. (2007). Weather and body condition in wintering mallards *Anas platyrhynchos*. *Bird*
698 *Study*, *54*(2), 154–159. https://doi.org/10.1080/00063650709461470

699 Brook, R. W., Ross, R. K., Abraham, K. F., Fronczak, D. L., & Davies, J. C. (2009). Evidence
700 for black duck winter distribution change. *Journal of Wildlife Management*, *73*(1), 98–103.
701 https://doi.org/10.2193/2007-424

702 Bruderer, B., & Boldt, A. (2008). Flight characteristics of birds: I. radar measurements of speeds.
703 *Ibis*, *143*(2), 178–204. https://doi.org/10.1111/j.1474-919X.2001.tb04475.x

704 Colwell, M. A., Taft O. W. (2000). Waterbird communities in managed wetlands of varying
705 water depth. *Waterbirds*, *23*, 45–55.

706 Cooper, C., Larson, L., Dayer, A., Stedman, R., & Decker, D. (2015). Are wildlife recreationists
707 conservationists? Linking hunting, birdwatching, and pro-environmental behavior. *The*
708 *Journal of Wildlife Management*, *79*(3), 446–457. https://doi.org/10.1002/jwmg.855

709 Dabbert, C. B., Martin, T. E., & Powell, K. C. (1997). Use of body measurements and serum
710 metabolites to estimate the nutritional status of mallards wintering in the Mississippi Alluvial
711 Valley, USA. *Journal of Wildlife Diseases*, *33*, 57-63.

712 Davis, B. E., Afton, A. D., and Cox Jr., R. R. (2011). Factors affecting winter survival of female
713 mallards in the lower Mississippi Alluvial Valley. *Waterbirds, 34*, 186-194.
714 Drent, R., Both, C., Green, M., Madsen, J., & Piersma, T. (2003). Pay-offs and penalties of
715 competing migratory schedules. *Oikos*, *103*(2), 274–292. https://doi.org/10.1034/j.1600-
716 0706.2003.12274.x
717 Drilling, N., Titman, R. D., & McKinney, F. (2020). Mallard, *Anas platyrhynchos*. Birds of the
718 World, Version: 1.0 — Published March 4, 2020.
719 Fredrickson, L. H., & Reid, F. A. (1988). Nutritional values of waterfowl foods. 13.1.1 in D. H.
720 Cross and P. Vohs (eds.) Waterfowl Management Handbook. U.S. Fish and Wildlife Service,
721 Fort Collins, Colorado, USA. http://www.nwrc.usgs.gov/wdb/pub/wmh/contents.html
722 (accessed 5 May 2016).
723 Fry, J., Xian G., Jin S., Dewitz J., Homer C., Yang L., Barnes C., Herold N., & Wickham J.
724 (2011). Completion of the 2006 National Land Cover Database for the Conterminous United
725 States. *Photogrammetric Engineering and Remote Sensing*, *77*, 858–864.
726 Gilbert, M., Xiao, X., Domenech, J., Lubroth, J., Martin, V., & Slingenbergh, J. (2006). Anatidae
727 migration in the Western Palearctic and spread of highly pathogenic avian influenza H5N1
728 virus. *Emerging Infectious Diseases*, *12*(11), 1650–1656.
729 https://doi.org/10.3201/eid1211.060223
730 Grado, S. C., Kaminski R. M., Munn I. A., & Tullos T. A. (2001). Economic impacts of
731 waterfowl hunting on public lands and at private lodges in the Mississippi Delta. *Wildlife*
732 *Society Bulletin*, *29*, 846-855.

733 Grimm, V., & Railsback S. F. (2012). Pattern-oriented modelling: a “multi-scope” for predictive
734 systems ecology. *Philosophical Transactions of the Royal Society B: Biological Sciences*,
735 *367*, 298–310.
736 Guillemain, M., Fritz, H., & Blais, S. (2000). Foraging methods can affect patch choice: an
737 experimental study in mallard (*Anas platyrhynchos*). *Behavioural Processes*, *50*(2–3), 123–
738 129. https://doi.org/10.1016/S0376-6357(00)00095-4
739 Gutierrez Illan, J., Wang, G., Cunningham, F. L., & King, D. T. (2017). Seasonal effects of wind
740 conditions on migration patterns of soaring American white pelican. *PLOS ONE*, *12*(10),
741 e0186948. https://doi.org/10.1371/journal.pone.0186948
742 Hagy, H. M., & Kaminski, R. M. (2012). Apparent seed use by ducks in moist-soil wetlands of
743 the Mississippi Alluvial Valley. *The Journal of Wildlife Management*, *76*(5), 1053–1061.
744 https://doi.org/10.1002/jwmg.325
745 Hansson, L.-A., & Åkesson, S. (2014). *Animal movement across scales*. Oxford: Oxford
746 University Press. Retrieved from
747 http://www.oxfordscholarship.com/view/10.1093/acprof:oso/9780199677184.001.0001/
748 acprof-9780199677184
749 Hartung, R. (1967). Energy metabolism in oil-covered ducks. *The Journal of Wildlife*
750 *Management*, *31*(4), 798. https://doi.org/10.2307/3797987
751 Harvell, C. D. (2002). Climate warming and disease risks for terrestrial and marine biota.
752 *Science*, *296*(5576), 2158–2162. https://doi.org/10.1126/science.1063699
753 Hedenström, A. (1992). Flight performance in relation to fuel load in birds. *Journal of*
754 *Theoretical Biology*, *158*(4), 535–537. https://doi.org/10.1016/S0022-5193(05)80714-3

Heitmeyer, M. E. (2010). A manual for calculating Duck-Use-Days to determine habitat resource values and waterfowl population energetic requirements in the Mississippi Alluvial Valley. Greenbrier Wetland Services Report 10-01. Prepared for the U.S. Army Corps of Engineers.

Holloway, P., and Miller, J. A. (2017). A quantitative sysnthesis of the movement concepts used within species distribution modelling. *Ecological Modelling*, *356*, 91-103.

Kalnay, E., Kanamitsu, M., Kistler, R., Collins, W., Deaven, D., Gandin, L., Iredell M., Saha S., White G., Woollen J., Zhu Y., Chelliah M., Ebisuzaki W., Higgins W., Janowiak J., Mo K. C., Ropelewski C., Wang J., Leetmaa A., Reynolds R., Jenne R., & Joseph, D. (1996). The NCEP/NCAR40-year reanalysis project. *Bulletin of the American Meteorological Society*, *77*(3), 437–471. https://doi.org/10.1175/1520-0477(1996)077<0437:TNYRP>2.0.CO;2

Kaminski, R. M., Davis, J. B., Essig, H. W., Gerard, P. D., & Reinecke, K. J. (2003). True metabolizable energy for wood ducks from acorns compared to other waterfowl foods. *The Journal of Wildlife Management*, *67*(3), 542. https://doi.org/10.2307/3802712

Kitamura, R., & Sperling, D. (1987). Refueling behavior of automobile drivers. *Transportation Research Part A: General*, *21*(3), 235–245. https://doi.org/10.1016/0191-2607(87)90017-3

Klaassen, M. (1996). Metabolic constraints on long-distance migration in birds. *The Journal of Experimental Biology*, *199*, 57–64.

Klaassen, M., Bauer, S., Madsen, J., & Tombre, I. (2005). Modelling behavioural and fitness consequences of disturbance for geese along their spring flyway. *Journal of Applied Ecology*, *43*(1), 92–100. https://doi.org/10.1111/j.1365-2664.2005.01109.x

Krapu, G. L. (1981). The role of nutrient reserves in mallard reproduction. *Auk, 98*, 28-38.

776 Krementz, D. G., Asante, K., & Naylor, L. W. (2011). Spring migration of mallards from
777 Arkansas as determined by satellite telemetry. *Journal of Fish and Wildlife Management*,
778 *2*(2), 156–168. https://doi.org/10.3996/042011-JFWM-026
779 Krementz, D. G., Asante, K., & Naylor, L. W. (2012). Autumn migration of Mississippi flyway
780 mallards as determined by satellite telemetry. *Journal of Fish and Wildlife Management*,
781 *3*(2), 238–251. https://doi.org/10.3996/022012-JFWM-019
782 La Sorte, F. A., & Thompson, F. R. (2007). Poleward shifts in winter ranges of North American
783 birds. *Ecology*, *88*(7), 1803–1812. https://doi.org/10.1890/06-1072.1
784 La Sorte, F. A., Fink, D., Hochachka, W. M., DeLong, J. P., & Kelling, S. (2013). Population-
785 level scaling of avian migration speed with body size and migration distance for powered
786 fliers. *Ecology*, *94*(8), 1839–1847. https://doi.org/10.1890/12-1768.1
787 La Sorte, F. A., Fink, D., Hochachka, W. M., DeLong, J. P., & Kelling, S. (2014a). Spring
788 phenology of ecological productivity contributes to the use of looped migration strategies by
789 birds. *Proceedings of the Royal Society B: Biological Sciences*, *281*(1793), 20140984–
790 20140984. https://doi.org/10.1098/rspb.2014.0984
791 La Sorte, F. A., Fink, D., Hochachka, W. M., Farnsworth, A., Rodewald, A. D., Rosenberg, K.
792 V., Kelling, S. (2014b). The role of atmospheric conditions in the seasonal dynamics of
793 North American migration flyways. *Journal of Biogeography*, *41*(9), 1685–1696.
794 https://doi.org/10.1111/jbi.12328
795 Lima, S. L. (1986). Predation risk and unpredictable feeding conditions: Determinants of body
796 mass in birds. *Ecology*, *67*, 377–385.

797 Lindström, Å. (2003). Fuel deposition rates in migrating birds: Causes, constraints and
798 consequences. In Avian Migration (eds. P. Berthold, E. Gwinner, E. Sonnenschein), pp 308 -
799 320. Springer-Verlag, Berlin, Germany.
800 Link, W. A., Sauer J. R., Niven D. K. (2006). A hierarchical model for regional analyses of
801 population change using Christmas Bird Count data, with application to the American black
802 duck. *Condor*, *108*, 13–24.
803 Lonsdorf, E. V., Thogmartin, W. E., Jacobi, S., Aagaard, K., Coppen, J., Davis, A., Fox T.,
804 Heglund P., Johnson R., Jones T., Kenow K., Lyons J., Luke K., Still S., & Tavernia, B.
805 (2016). A generalizable energetics-based model of avian migration to facilitate continental-
806 scale waterbird conservation. *Ecological Applications*, *26*(4), 1136–1153.
807 https://doi.org/10.1890/14-1947
808 López-Hoffman, L., Chester C. C., Semmens D. J., Thogmartin W. E., Rodriguez McGoffin M.
809 S., Merideth R., Diffendorfer J. E. (2017). Ecosystem services from trans-border migratory
810 species: implications for conservation governance. *Annual Reviews of Environment and*
811 *Resources*, *42*, 509–539.
812 Louchart, A. (2008). Emergence of long distance bird migration: A new model integrating global
813 climate changes. *Naturwissenschaften*, **95**, 1109–1119.
814 Marra, P. P., Cohen, E. B., Loss, S. R., Rutter, J. E., & Tonra, C. M. (2015). A call for full
815 annual cycle research in animal ecology. *Biology Letters*, *11*(8), 20150552.
816 https://doi.org/10.1098/rsbl.2015.0552
817 Mattsson, B. J., Dubovsky, J. A., Thogmartin, W. E., Bagstad, K. J., Goldstein, J. H., Loomis, J.
818 B., Diffendorfer J. E., Semmens D. J., Wiederholt R., & López-Hoffman, L. (2018).
819 Recreation economics to inform migratory species conservation: Case study of the northern

820 pintail. *Journal of Environmental Management*, *206*, 971–979.
821 https://doi.org/10.1016/j.jenvman.2017.11.048
822 Mattsson, B. J., Devries, J. H., Dubovsky, J. A., Semmens, D., Thogmartin, W. E., Derbridge, J.
823 J. & López-Hoffman, L. (2020). Sources and dynamics of international funding for
824 waterfowl conservation in the Prairie Pothole Region of North America. *Wildlife Research*,
825 *47*, 279–295. https://doi.org/10.1071/WR19100
826 Moore, T. T. (2011). Climate change and animal migration. *Environmental Law*, *41*, 393–405.
827 Newton, I. (2006). Can conditions experienced during migration limit the population levels of
828 birds? *Journal of Ornithology*, *147*(2), 146–166. https://doi.org/10.1007/s10336-006-0058-4
829 Newton, I., & Brockie, K. (2008). *The migration ecology of birds*. Amsterdam: Elsevier/Acad.
830 Press.
831 Nichols, J. D., Reinecke K. J., Hines J. E. (1983) Factors affecting the distribution of mallards
832 wintering in the Mississippi Alluvial Valley. *The Auk*, *100*, 932–946.
833 Notaro, M., Lorenz, D., Hoving, C., & Schummer, M. (2014). Twenty-first-century projections
834 of snowfall and winter severity across central-eastern North America. *Journal of Climate*,
835 *27*(17), 6526–6550. https://doi.org/10.1175/JCLI-D-13-00520.1
836 Notaro, M., Zhong Y., Vavrus S., Schummer M. L., Van Den Elsen L. M., Coluccy J. M.,
837 Hoving C. (2016). Projected influences of changes in weather severity on autumn and winter
838 distributions of dabbling ducks in the Mississippi and Atlantic Flyways during the twenty-
839 first century. *PLoS ONE*, *11*, e0167506.
840 Owen, M., & W. A. Cook. (1977). Variations in body weight, wing length and condition of
841 Mallard *Anas platyrhynchos* and their relationship to environmental changes. *Journal of*
842 *Zoology*, *182*, 377–395.

843 Parmesan, C. (2006). Ecological and evolutionary responses to recent climate change. *Annual*
844 *Review of Ecology, Evolution, and Systematics*, *37*(1), 637–669.
845 https://doi.org/10.1146/annurev.ecolsys.37.091305.110100
846 Paxton, K. L., Cohen, E. B., Paxton, E. H., Németh, Z., & Moore, F. R. (2014). El Niño-
847 Southern Oscillation is linked to decreased energetic condition in long-distance migrants.
848 *PLoS ONE*, *9*(5), e95383. https://doi.org/10.1371/journal.pone.0095383
849 Pearse, A. T., Kaminski, R. M., Reinecke, K. J., & Dinsmore, S. J. (2012). Local and landscape
850 associations between wintering dabbling ducks and wetland complexes in Mississippi.
851 *Wetlands*, *32*, 859–869.
852 Pennycuick, C. J. (1975). Mechanics of Flight. In Avian Biology, vol. 5 (ed. D. S. Farner, and J.
853 R. King), pp. 1–75. Academic Press, London, UK.
854 Pennycuick, C. J. (2008). Modelling the Flying Bird. Elsevier (Academic Press), Burlington,
855 MA, USA.
856 Pennycuick, C. J., Akesson, S., & Hedenstrom, A. (2013). Air speeds of migrating birds
857 observed by ornithodolite and compared with predictions from flight theory. *Journal of The*
858 *Royal Society Interface*, *10*(86), 20130419–20130419. https://doi.org/10.1098/rsif.2013.0419
859 Pennycuick, C. J., & Battley, P. F. (2003). Burning the engine: a time-marching computation of
860 fat and protein consumption in a 5420-km non-stop flight by great knots, *Calidris*
861 *tenuirostris*. *Oikos*, *103*(2), 323–332. https://doi.org/10.1034/j.1600-0706.2003.12124.x
862 Prince, H. H. (1979). Bioenergetics of postbreeding dabbling ducks. In Waterfowl and wetlands
863 – an integrated review (ed. T. A. Bookhout), pp. 103–117. University of Wisconsin –
864 Madison, Madison, Wisconsin, USA.

R Core Team (2018). R: A language and environment for statistical computing. R Foundation for Statistical Computing, Vienna, Austria. URL https://www.R-project.org/.

Rayner, J. (1990). The mechanics of flight and bird migration performance. In Bird Migration (ed. E. Gwinner), pp. 283–299. Springer-Verlag, Heidelberg, Germany.

Ricklefs, R. E. (1977). Composition of Eggs of Several Bird Species. *Auk, 94*, 350–356, https://doi.org/10.1093/auk/94.2.350

Ridgley, R. S., Allnutt T. F., Brooks T., McNicol D. K., Mehlman D. W., Young B. E., Zook J. R. (2005). Digital distribution maps of the birds of the Western Hemisphere, version 2.1. NatureServe, Arlington, Virginia, USA.

Robinson, O. J., McGowan, C. P., & Devers, P. K. (2016). Updating movement estimates for American black ducks (*Anas rubripes*). *PeerJ*, *4*, e1787. https://doi.org/10.7717/peerj.1787

Schummer, M. L., Kaminski, R. M., Raedeke, A. H., & Graber, D. A. (2010). Weather-related indices of autumn–winter dabbling duck abundance in middle North America. *Journal of Wildlife Management*, *74*(1), 94–101. https://doi.org/10.2193/2008-524

Schummer, M. L., Coluccy, J. M., Mitchell, M., & Van Den Elsen, L. (2017). Long-term trends in weather severity indices for dabbling ducks in eastern North America: Internet *WSI* Tool. *Wildlife Society Bulletin*, *41*(4), 615–623. https://doi.org/10.1002/wsb.837

Smith, K. G., Prince H. H. (1973). The fasting metabolism of subadult mallards acclimatized to low ambient temperatures. *The Condor*, *75*, 330–335.

Sotherland, P. R., & Rahn, H. (1987). On the composition of bird eggs. *The Condor, 89*, 48-65, https://doi.org/10.2307/1368759

886 Stanley, C. Q., MacPherson, M., Fraser, K. C., McKinnon, E. A., & Stutchbury, B. J. M. (2012).
887 Repeat tracking of individual songbirds reveals consistent migration timing but flexibility in
888 route. *PLoS ONE*, *7*(7), e40688. https://doi.org/10.1371/journal.pone.0040688
889 Stirnemann, R. L., O'Halloran, J., Ridgway, M., & Donnelly, A. (2012). Temperature-related
890 increases in grass growth and greater competition for food drive earlier migrational departure
891 of wintering Whooper Swans: Drivers of migration in Whooper Swan. *Ibis*, *154*(3), 542–553.
892 https://doi.org/10.1111/j.1474-919X.2012.01230.x
893 Tingley, M. W., Monahan W. B., Beissinger S. R., Moritz C. (2009). Birds track their
894 Grinnellian niche through a century of climate change. *Proceedings of the National Academy*
895 *of Sciences USA*, *106*, 19637–19643.
896 U.S. Fish and Wildlife Service. (2013). Final Environmental Impact Statement on resident
897 Canada good management. U.S. Department of the Interior, Washington, D.C., USA. https://
898 www.fws.gov/migratorybirds/pdf/surveys-and-data/Final_EIS_Resident_CAGO_with_Appe
899 ndices.pdfU.S. Fish and Wildlife Service. 2013. Waterfowl population status. 2013. U.S.
900 Department of the Interior, Washington, D.C., USA.
901 Vaananen, V. M. (2001). Hunting disturbance and the timing of autumn migration in Anas
902 species. *Wildlife Biology*, *7*, 3–9.
903 Van Den Elsen, L. M. (2016). Weather and photoperiod indices of autumn and winter dabbling
904 duck abundance in the Mississippi and Atlantic flyways of North America. University of
905 Western Ontario, Electronic Thesis and Dissertation Repository. 3642.
906 https://ir.lib.uwo.ca/etd/3642.

907 Walther, G.-R., Post, E., Convey, P., Menzel, A., Parmesan, C., Beebee, T. J. C., Fromentin J.-
908 M., Hoegh-Guldberg O., & Bairlein, F. (2002). Ecological responses to recent climate
909 change. *Nature*, *416*(6879), 389–395. https://doi.org/10.1038/416389a
910 Zimmer, C., Boos, M., Petit, O., & Robin, J.-P. (2010). Body mass variations in disturbed
911 mallards *Anas platyrhynchos* fit to the mass-dependent starvation-predation risk trade-off.
912 *Journal of Avian Biology, 41*, 637-644.

Tables

Table 1. Definition, values, and units for each parameter used in the model.

Parameter	Definition	Value	Units
d	Local movement distance	3,000	m
v	Mean flight velocity	76 – 86	km/hr
e	Energetic cost of flight (per hr)	0.042 – 0.076	kJ/hr
w	Weather Severity Index threshold	7.5	—
r	Flight range	2,253	km
n	Node size	32.187	km
N_0	Initial population size	19,856,514	individuals
m	Body mass	800 – 1,300	grams
LCT	Lower Critical Temperature	$47.2 \times (m \times 1000)^{-0.18}$	°C
s_d	Daily survivorship range	0.9975 – 0.9997	—
f	Proportional body fat range	0 – 0.13	—

916 **Table 2**. Values assigned to the weights for natural forage decay rates in available land cover
917 classes.

Land cover class	Weight
Shoreline	0.9998
Crops	0.9970
Woody wetlands	0.9965
Herbaceous wetlands	0.9910

918

Figure Legends

Figure 1. Graphical representation of the order of operations of the model. We initiated (1) foraging activity (i.e., the loss of forage material from the habitat as a result of active foraging and natural decay and the subsequent acquisition of the actively foraged material to augment body condition, **BC**) prior to (2) departure, the probability of which was dictated by the node-specific weather severity index (***WSI***), class-specific **BC**, distance between a focal node and the nearest breeding node (distance to breeding grounds, **DB**), and the node-specific air density (**AD**). Arrival of individuals (3) followed, informed by node-specific forage quantity (**F**), roosting habitat quality (**R**), cumulative gamma-movement probability (the probability of moving between each pair of nodes on the landscape, given the distance between them; **G**), as well as **AD** and **DB**. Individuals were then redistributed among **BC** classes according to energy expended in flight and were redistributed spatially based on to-from node flights. Finally, the population incurred mortality (4) according to survivorship rates related to each **BC**. We calculated the number of individuals per body condition after mortality and arrival, as well as the number of individuals per node, for the following day.

Figure 2. Graphical representation of exponential weights for each of the four components of the Cobb-Douglas function used to define node attractiveness over time: amount of forage availability, air density, proportion of roosting habitat in each node, distance to the nearest breeding node, and a cumulative probability of moving to a node from all other nodes based on a gamma function.

941 **Figure 3**. An example of the abundance-weighted center-of-mass for the population on the 50th
942 day of migration, represented by the black dot. The gray shaded areas represent the top 2% most
943 populace nodes on day 50.
944
945 **Figure 4**. (A) Normalized $\left(\frac{x_i - \overline{x}}{sd(x)}\right)$ minimum available habitat on the landscape as a function of
946 normalized weather severity index (*WSI*); (B) Normalized mortality during the nonbreeding
947 period (September to May) as a function of normalized minimum available habitat; and (C)
948 Normalized mortality as a function of normalized *WSI*. Black lines indicate the line of best fit of
949 a generalized linear model and associated standard error (gray shaded area).
950
951 **Figure 5**. (A) Mean weather severity index (*WSI*; Schummer et al. 2010) within the available
952 habitat (areas with $WSI < 7.5$) and (B) across the entire landscape showed differing patterns over
953 time.
954
955 **Figure 6.** The standard deviation in the annual mean weather severity index (*WSI*) over the
956 period of record (1957 – 2019) for each node in North America. Mid-latitude and above areas
957 were subject to greater variation in weather severity over time than southerly areas, which are
958 more consistently incorporated in "available habitat" (areas with $WSI < 7.5$).
959
960 **Figure 7**. Map showing the 2% most populace nodes, in gray, across the nonbreeding period
961 (September to May) for all years (1957 – 2019). The darker the gray the more often a node
962 occurred within the 2% most populace nodes across the record. The 2% most populace nodes
963 were similar across most years, hence the consistent patches. Lines represent the path of the

964 abundance-weighted population center of mass, or migration route, across years, with the mean
965 of all years in black.
966
967 **Figure 8.** The mean distance among all abundance-weighted center-of-mass locations for the
968 population on each day increased as the standard deviation of the daily proportion of available
969 habitat (weather severity index < 7.5) increased.
970
971 **Figure 9**. Mean daily mortality (total number of dead birds) on each day of the non-breading
972 period across the period of record (1957 – 2019).
973
974 **Figure 10.** Comparison of mean daily proportion of available habitat during the nonbreeding
975 period for years in the highest quartile of mean annual weather severity index values ("Severe";
976 1961, 1964, 1966, 1971, 1972, 1974, 1975, 1977, 1978, 1981, 1982, 1984, 1993, 1995, 1996,
977 2013) and for years in the lower quartile ("Mild"; 1979, 1980, 1997, 1998, 1999, 2001, 2003,
978 2004, 2005, 2006, 2009, 2011, 2015, 2016, 2017).
979

980 **Figure 1.**

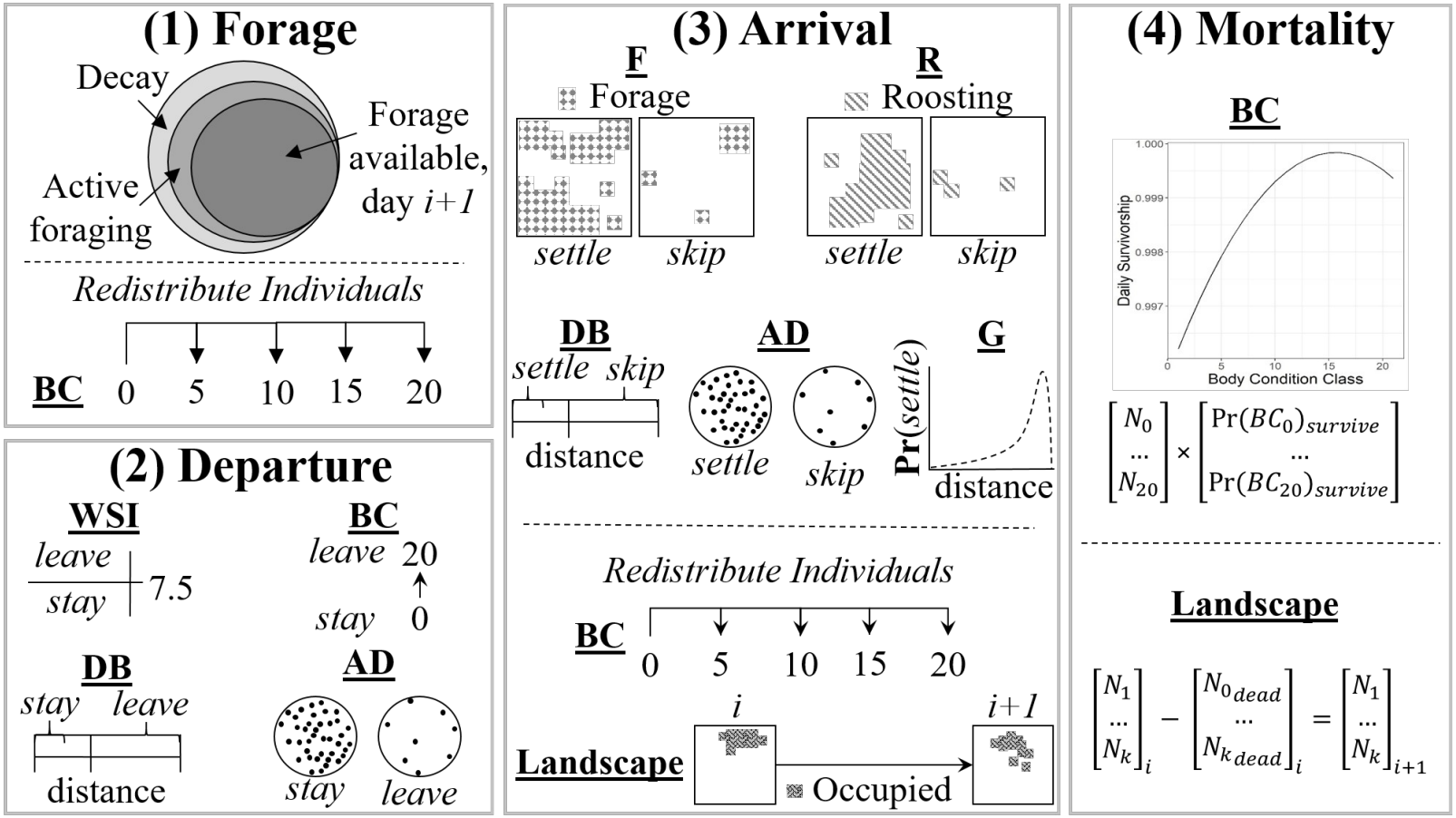

981

982 **Figure 2.**

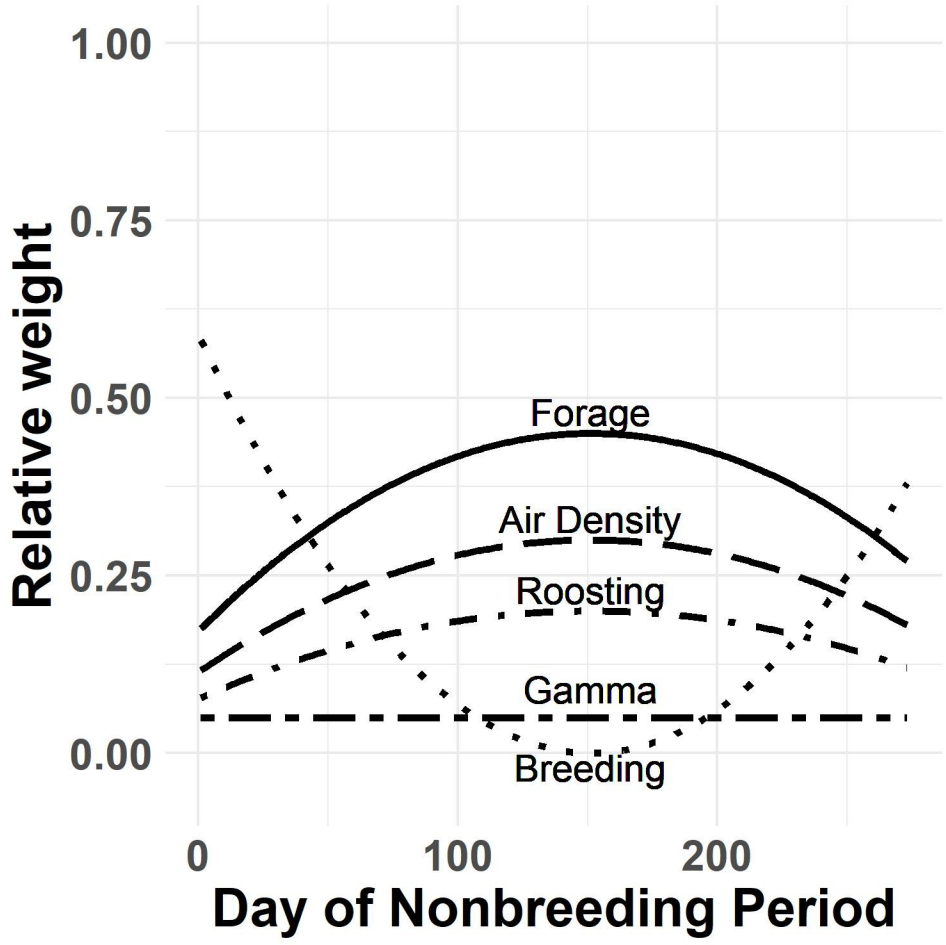

983

984 **Figure 3**.

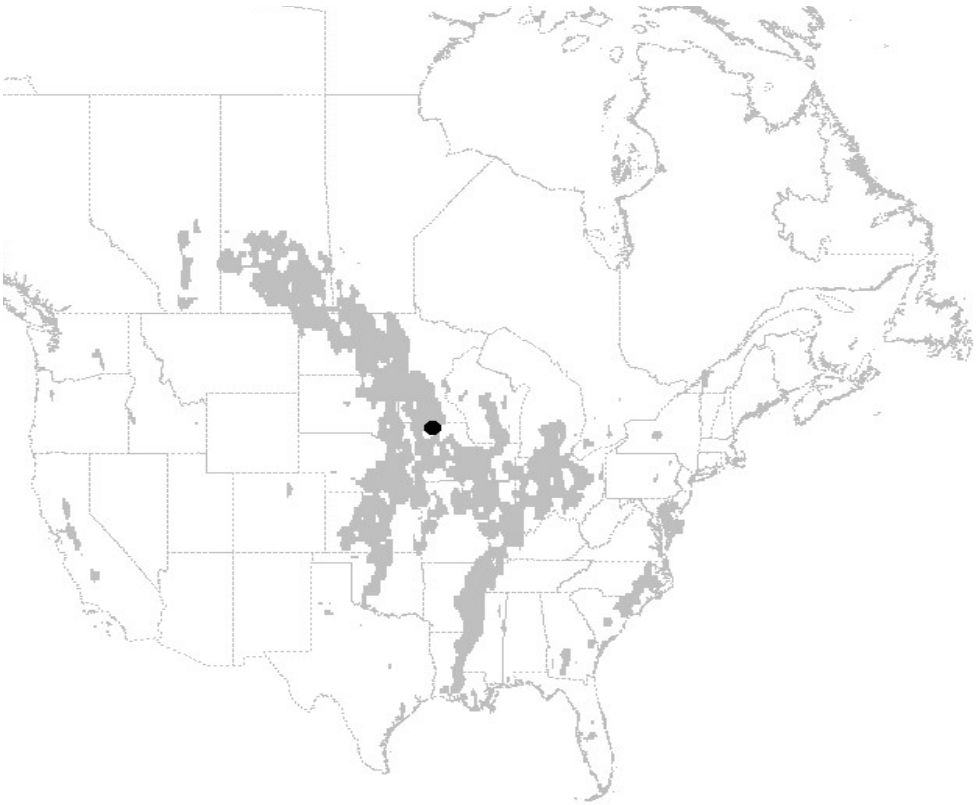

985

Figure 4.

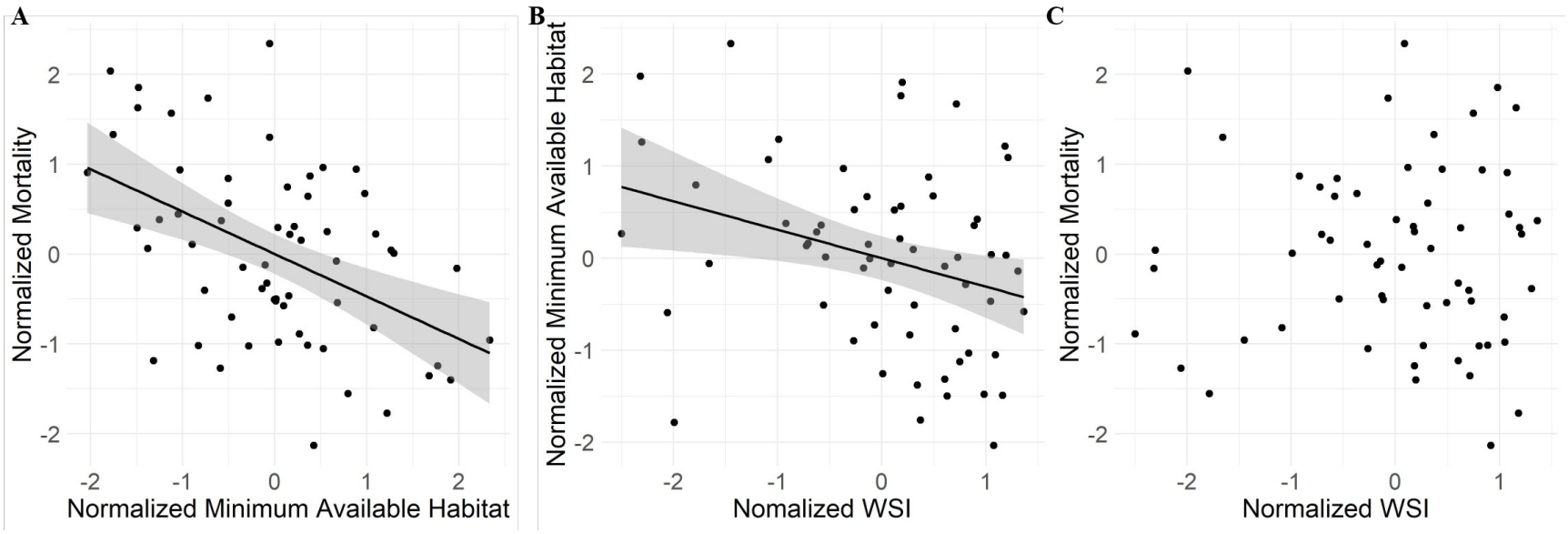
A
Normalized Mortality
Normalized Minimum Available Habitat
B
Normalized Minimum Available Habitat
Nomalized WSI
C
Normalized Mortality
Normalized WSI

989 **Figure 5.**

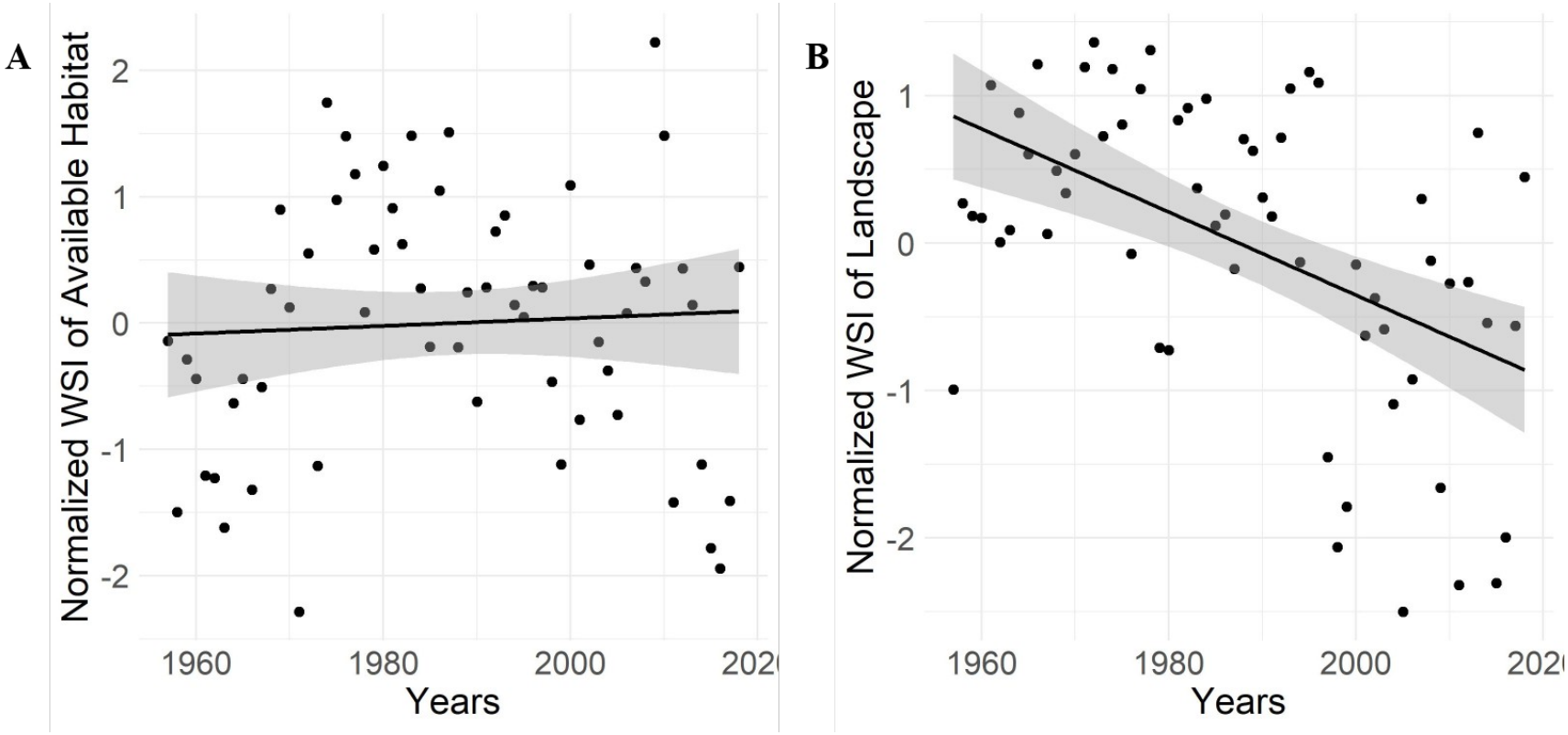

990

991 **Figure 6.**

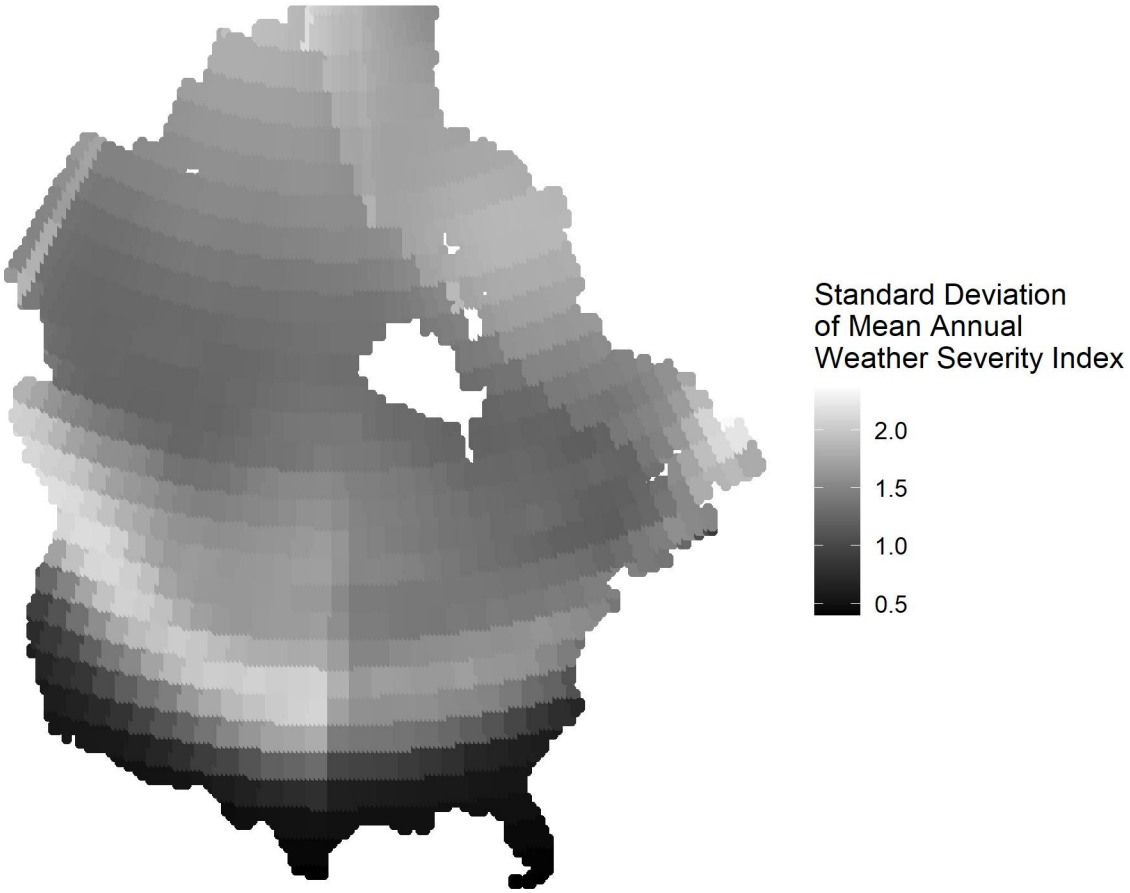

992

993

994 **Figure 7.**

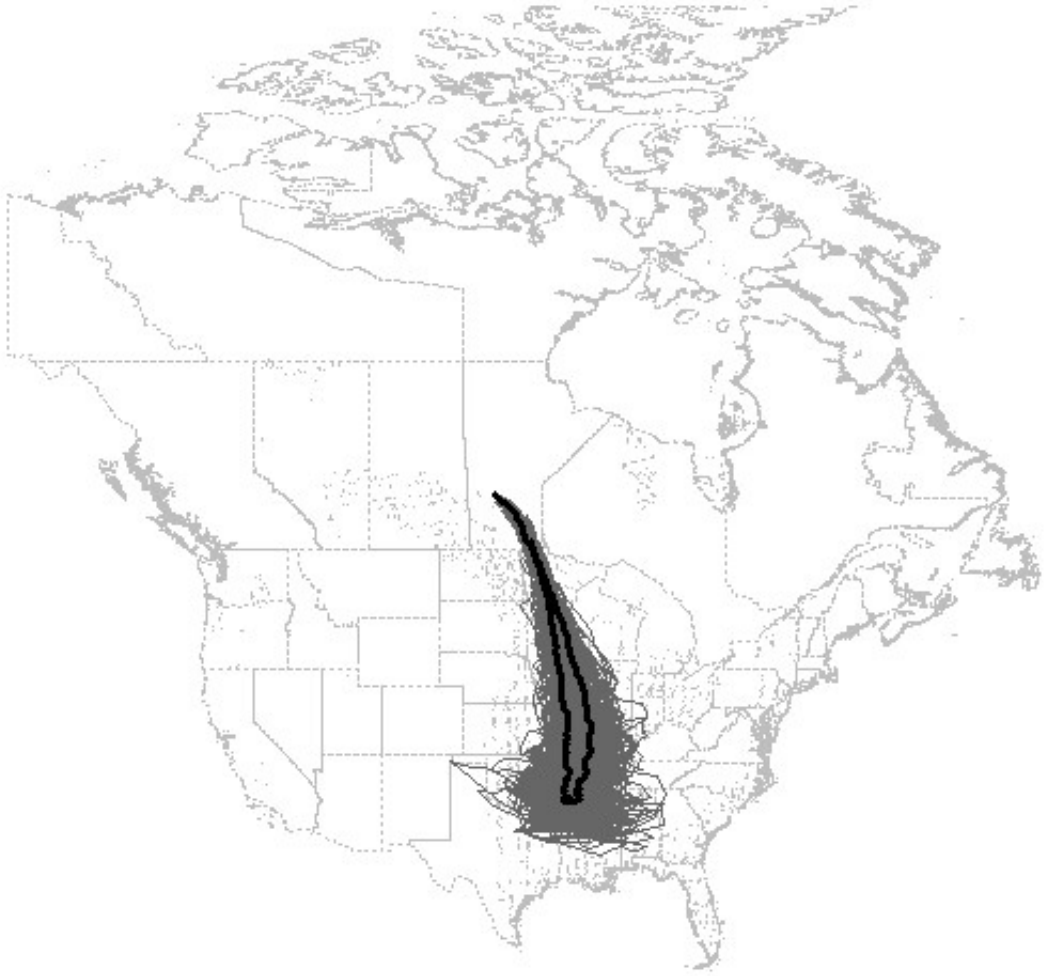

995

996

997 **Figure 8.**

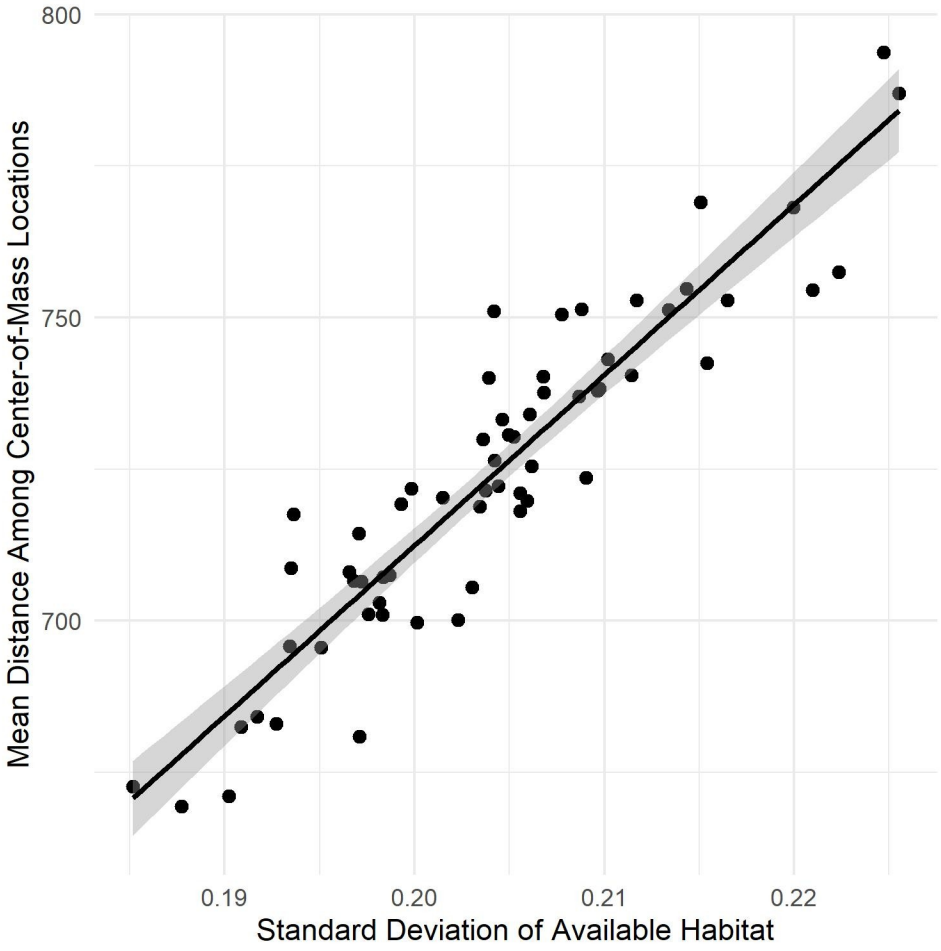

998

999

1000 **Figure 9.**

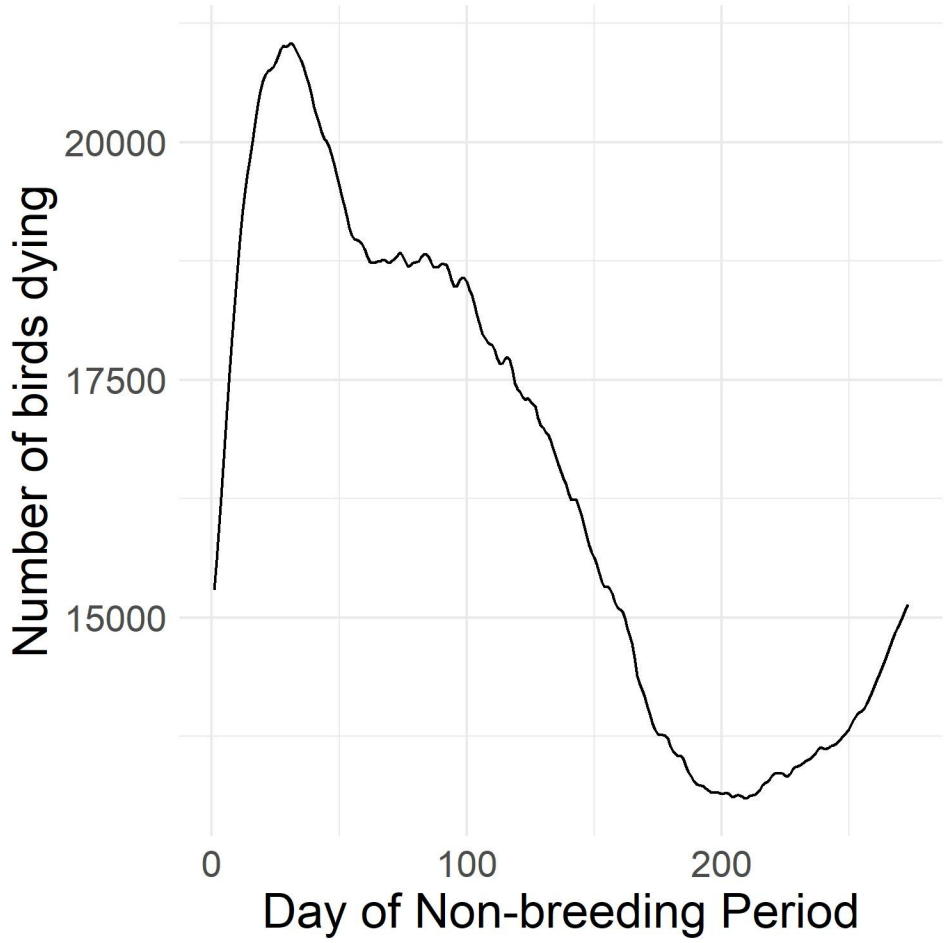

1001

1002 **Figure 10.**

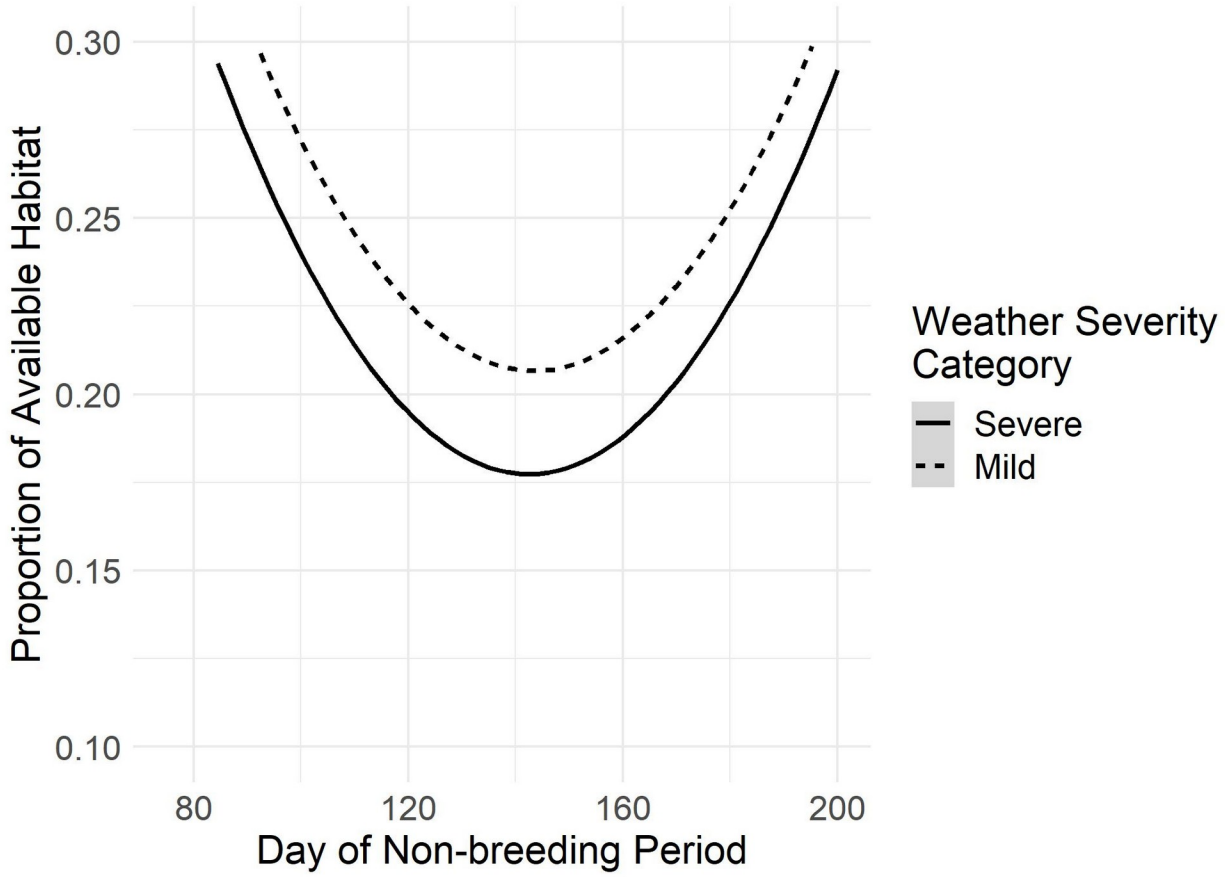

1003

1004

Supporting Material

We provide several files of supporting material for visualization of our results and replication of our methods.

File S1. (game_distrib.R) – R script used to apply the model and generate the results.

File S3. (weather_severity_index.R) – R script used to acquire the data and perform the calculations to generate the weather severity index for each day of the simulations.

File S4. (DailyAbundance_2013.gif) – A video showing the daily abundance per node across the landscape, normalized on a zero-to-one scale. White to gray dots depict the population-weighted center of mass on each day of migration to demonstrate an estimate of the population-level "migration path".

Appendix S1. Details of the cleaning, conversion, and projection of the weather data from the National Oceanic and Atmospheric Administration's National Centers for Environmental Prediction.

We used the RNCEP package (R-connection to National Centers for Environmental Prediction data; Kemp et al. 2012) to gather and manipulate the target climate data, which included data for each day between 1957 and 2019. We gathered air temperature (°K at 2 m above surface level), water equivalent of snow depth ($\frac{kg}{m^2}$ at surface level), and air pressure (Pascals at low cloud bottom) data sampled on a T62 Gaussian grid. We restricted data to the nonbreeding period, from 1 July of one calendar year to 31 May of the next (ignoring leap days). We converted air temperature to °C and water equivalent of snow depth to meters. To convert air pressure to density ($\frac{kg}{m^3}$), we divided the pressure by the product of the specific gas constant for dry air (287.058 $\frac{J}{kg*km}$) and air temperature.

The water equivalent of snow depth (or, snow-water equivalent, SWE) measures the amount of water that would be released by a volume of snow melting. It is calculable as the product of snow depth and snow density. To acquire snow depth (in m) given SWE, we took the quotient of SWE ($\frac{kg}{m^2}$) and snow density ($\frac{kg}{m^3}$). Snow density varies with temperature, and pressure (or depth, with snow deeper in a column being more compacted and thus denser). Snow density ranges from 10 to 400 $\frac{kg}{m^3}$ in our conditions (i.e., the temperatures observed across the focal landscape);

we assume a constant snow density of 400 $\frac{kg}{m^3}$ across the landscape to convert SWE to snow depth.

References

Kemp, M. U., E. Emiel van Loon, J. Shamoun-Baranes, and W. Bouten. 2012. RNCEP: global weather and climate data at your fingertips. Methods in Ecology and Evolution 3:65–70.

Appendix S2. Cross-walk of Canada (CSC2000v, Center for Topographic Information, Earth Sciences Sector and Natural Resources Canada 2009) and U.S. (National Land Cover Database 2006, Fry et al. 2011) land cover.

CSC Value	CSC Class	NLCD Value	NLCD Class
0	No Data	No Data	
10	Unclassified	No Data	
11	Cloud	No Data	
12	Shadow	No Data	
20	Water	11	Open Water
30	Barren	31	Barren Land
31	Snow/Ice	12	Perennial Ice/Snow
32	Rock/Rubble	31	Barren Land
33	Exposed Land	31	Barren Land
34	Developed	23	Developed, Medium Intensity
35	Sparsely vegetated bedrock	31	Barren Land
36	Sparsely vegetated till-colluvium	31	Barren Land
37	Bare soil with cryptogam crust - frostboils	31	Barren Land
40	Bryoids	74	Moss
50	Shrubland	52	Shrub/Scrub
51	Shrub -Tall	52	Shrub/Scrub
52	Shrub - Low	51	Dwarf Scrub
53	Prostrate dwarf shrub	51	Dwarf Scrub

80	Wetland	95	Emergent Herbaceous Wetlands
81	Wetland Treed	90	Wood Wetlands
82	Wetland Shrub	90	Wood Wetlands
83	Wetland Herb	95	Emergent Herbaceous Wetlands
100	Herb	71	Grassland/Herbaceous
101	Tussock graminoid tundra	72	Sedge/Herbaceous
102	Wet sedge	72	Sedge/Herbaceous
103	Moist to dry non-tussock graminoid/dwarf shrub tussock	51	Dwarf Scrub
104	Dry graminoid prostrate dwarf shrub tundra	51	Dwarf Scrub
110	Grassland	71	Grassland/Herbaceous
120	Cultivated agricultural land	82	Cultivated Crops
121	Annual crops	82	Cultivated Crops
122	Perennial crops and Pasture	81	Pasture/Hay
210	Coniferous	42	Evergreen Forest
211	Coniferous - Dense	42	Evergreen Forest
212	Coniferous - Open	42	Evergreen Forest
213	Coniferous - Sparse	42	Evergreen Forest
220	Broad Leaf	41	Deciduous Forest
221	Broad Leaf - Dense	41	Deciduous Forest
222	Broad Leaf - Open	41	Deciduous Forest
223	Broad Leaf - Sparse	41	Deciduous Forest

230	Mixed Wood	43	Mixed Forest
231	Mixed Wood - Dense	43	Mixed Forest
232	Mixed Wood - Open	43	Mixed Forest
233	Mixed Wood - Sparse	43	Mixed Forest

References

Center for Topographic Information, Earth Sciences Sector and Natural Resources Canada. 2009. Land cover, circa 2000-vector: Feature catalogue, edition 1.0. Geobase, http://www.geobase.ca/geobase/en/data/landcover/csc2000v/description.html.

Fry, J., G. Xian, S. Jin, J. Dewitz, C. Homer, L. Yang, C. Barnes, N. Herold, and J. Wickham. 2011. Completion of the 2006 National Land Cover Database for the Conterminous United States. Photogrammetric Engineering and Remote Sensing 77:858–864.

Appendix S3. Here we report several results and findings relevant to the change in weather severity over time and the subsequent effects of this change on the nadir of the latitudinal reach of the population each year.

Figure S3.1. The proportion of the landscape available for individuals to occupy on each day of the nonbreeding period, according to the weather severity index (*WSI*) in that node. *WSI* values above 7.5 trigger departure and inhibit arrival. This metric is normalized to a 0 to 1 scale for comparison across all years in the record (1957 – 2019).

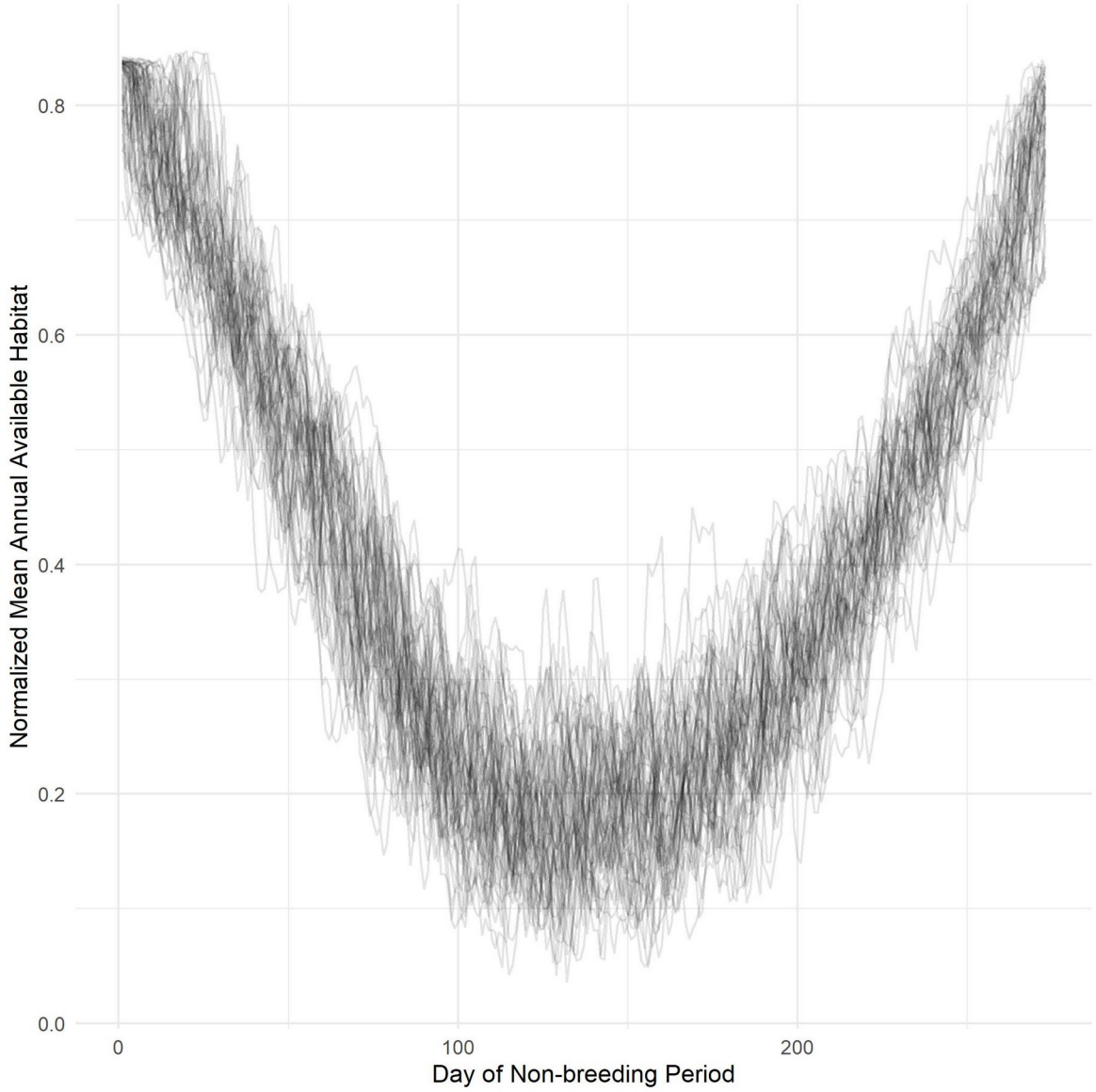

Figure S3.2. Change in the southernmost latitude achieved by the abundance-weighted center-of-mass of the population over time, with corresponding annual median weather severity index. Years of less severe weather (lighter curves) demonstrated less southerly minimum latitudes.

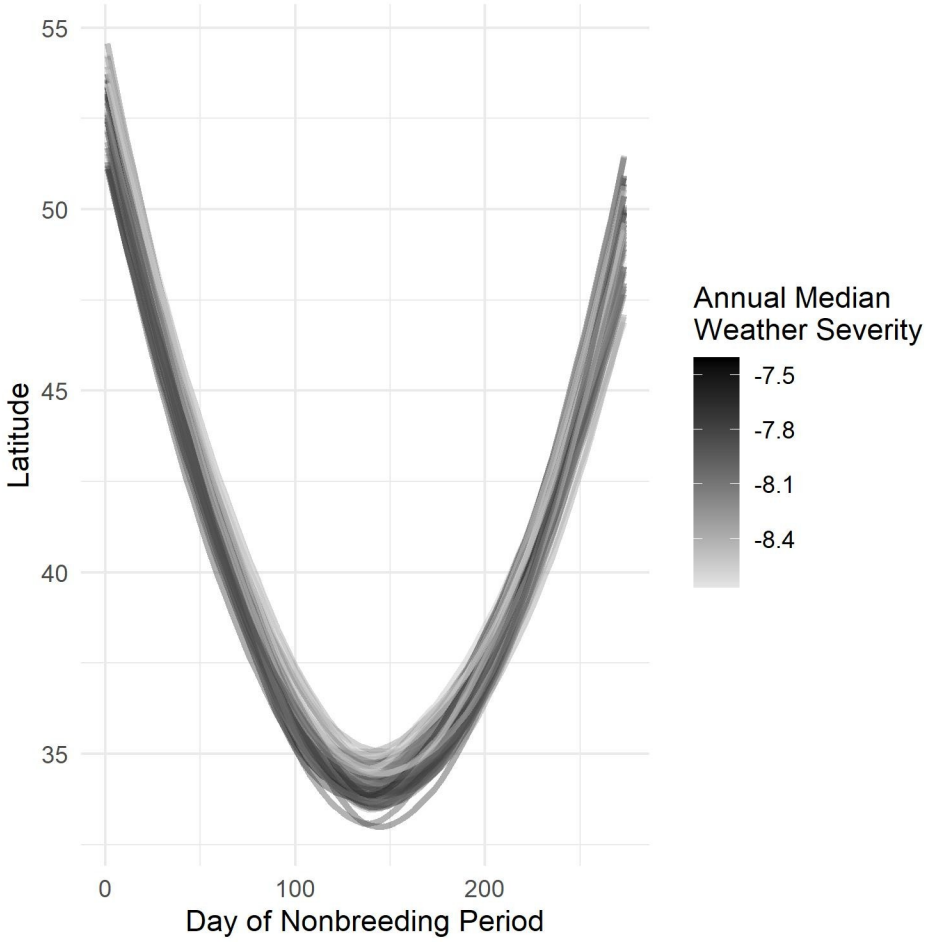

Figure S3.3. Change in the southernmost latitude achieved by the abundance-weighted center-of-mass of the population with varying annual median weather severity index values.